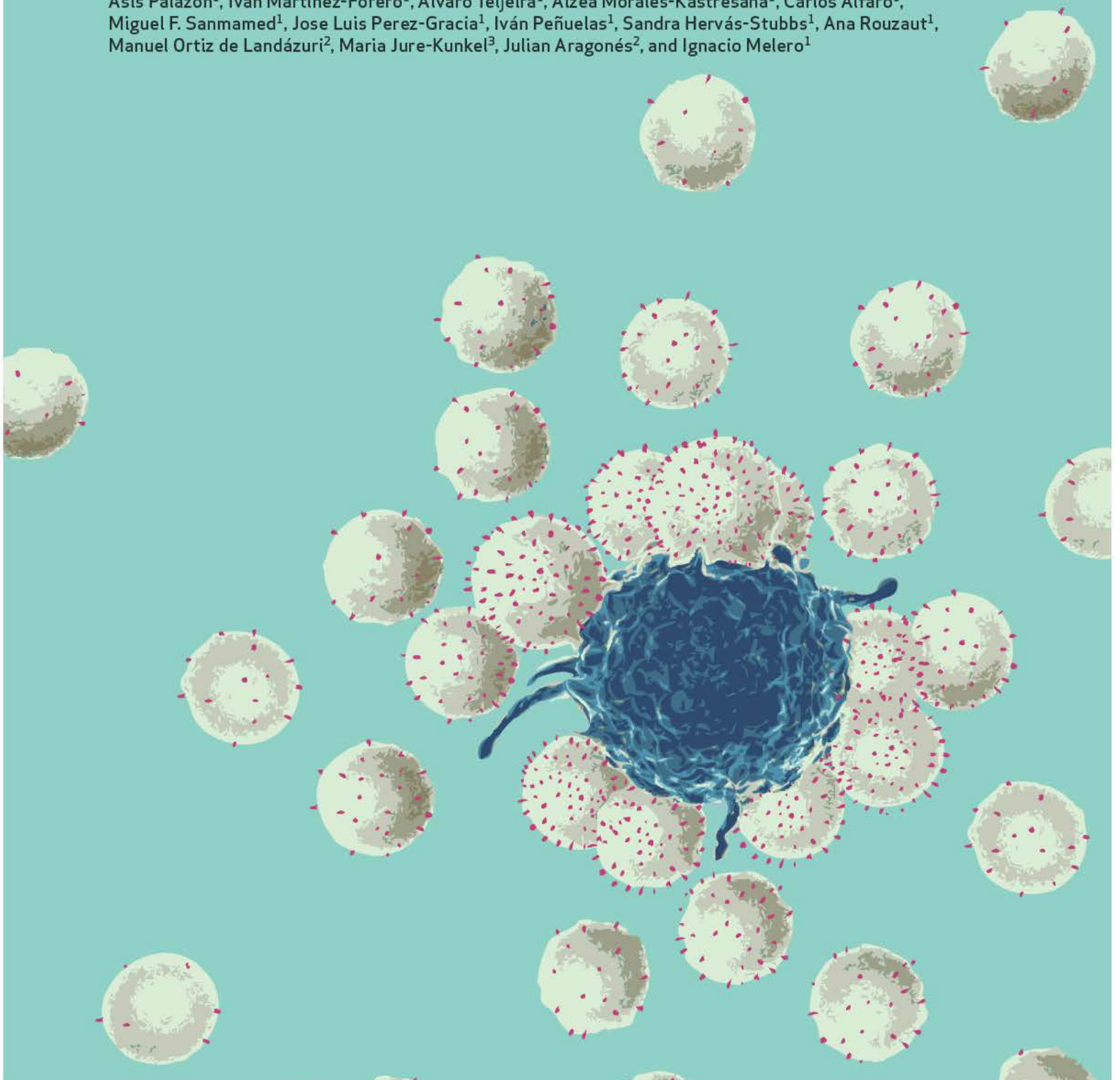


RESEARCH ARTICLE

# The HIF-1 $\alpha$ Hypoxia Response in Tumor-Infiltrating T Lymphocytes Induces Functional CD137 (4-1BB) for Immunotherapy

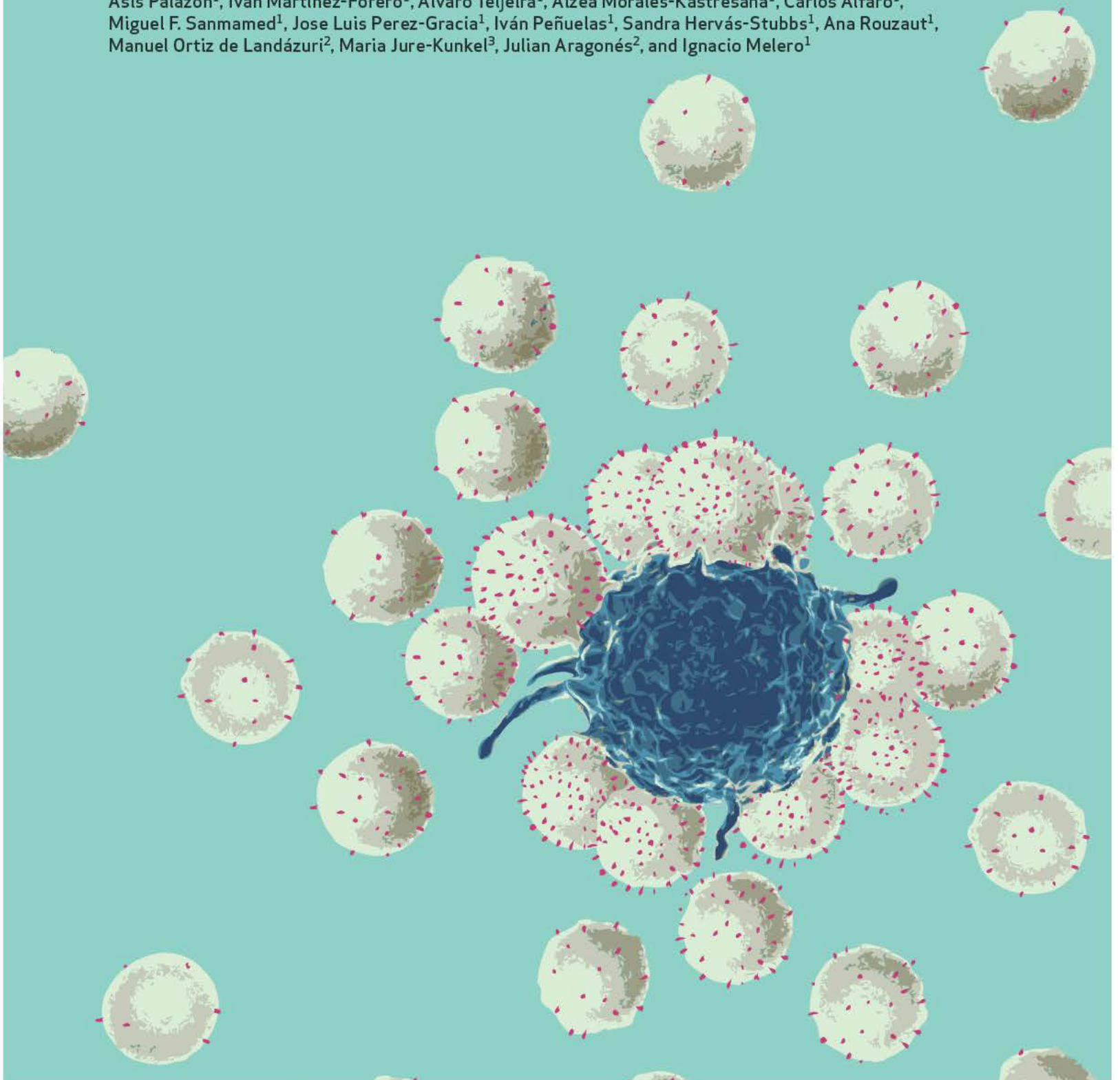
Asís Palazón<sup>1</sup>, Iván Martínez-Forero<sup>1</sup>, Alvaro Teijeira<sup>1</sup>, Aizea Morales-Kastresana<sup>1</sup>, Carlos Alfaro<sup>1</sup>, Miguel F. Sanmamed<sup>1</sup>, Jose Luis Perez-Gracia<sup>1</sup>, Iván Peñuelas<sup>1</sup>, Sandra Hervás-Stubbs<sup>1</sup>, Ana Rouzaut<sup>1</sup>, Manuel Ortiz de Landázuri<sup>2</sup>, Maria Jure-Kunkel<sup>3</sup>, Julian Aragonés<sup>2</sup>, and Ignacio Melero<sup>1</sup>



RESEARCH ARTICLE

# The HIF-1 $\alpha$ Hypoxia Response in Tumor-Infiltrating T Lymphocytes Induces Functional CD137 (4-1BB) for Immunotherapy

Asís Palazón<sup>1</sup>, Iván Martínez-Forero<sup>1</sup>, Alvaro Teijeira<sup>1</sup>, Aizea Morales-Kastresana<sup>1</sup>, Carlos Alfaro<sup>1</sup>, Miguel F. Sanmamed<sup>1</sup>, Jose Luis Perez-Gracia<sup>1</sup>, Iván Peñuelas<sup>1</sup>, Sandra Hervás-Stubbs<sup>1</sup>, Ana Rouzaut<sup>1</sup>, Manuel Ortiz de Landázuri<sup>2</sup>, Maria Jure-Kunkel<sup>3</sup>, Julian Aragonés<sup>2</sup>, and Ignacio Melero<sup>1</sup>



**ABSTRACT**

The tumor microenvironment of transplanted and spontaneous mouse tumors is profoundly deprived of oxygenation as confirmed by positron emission tomographic (PET) imaging. CD8 and CD4 tumor-infiltrating T lymphocytes (TIL) of transplanted colon carcinomas, melanomas, and spontaneous breast adenocarcinomas are CD137 (4-1BB)-positive, as opposed to their counterparts in tumor-draining lymph nodes and spleen. Expression of CD137 on activated T lymphocytes is markedly enhanced by hypoxia and the prolyl-hydroxylase inhibitor dimethylxalylglycine (DMOG). Importantly, hypoxia does not upregulate CD137 in hypoxia-inducible factor (HIF)-1 $\alpha$ -knockout T cells, and such HIF-1 $\alpha$ -deficient T cells remain CD137-negative even when becoming TILs, in clear contrast to co-infiltrating and co-transferred HIF-1 $\alpha$ -sufficient T lymphocytes. The fact that CD137 is selectively expressed on TILs was exploited to confine the effects of immunotherapy with agonist anti-CD137 monoclonal antibodies to the tumor tissue. As a result, low-dose intratumoral injections avoid liver inflammation, achieve antitumor systemic effects, and permit synergistic therapeutic effects with PD-L1/B7-H1 blockade.

**SIGNIFICANCE:** CD137 (4-1BB) is an important molecular target to augment antitumor immunity. Hypoxia in the tumor microenvironment as sensed by the HIF-1 $\alpha$  system increases expression of CD137 on tumor-infiltrating lymphocytes that thereby become selectively responsive to the immunotherapeutic effects of anti-CD137 agonist monoclonal antibodies as those used in ongoing clinical trials. *Cancer Discov*; 2(7): 608–23. ©2012 AACR.

**INTRODUCTION**

The study of immune cells in culture is routinely conducted under 21% O<sub>2</sub> concentrations. However, in the tissues where immune responses take place, the concentration of O<sub>2</sub> is much lower (1). This is true in secondary lymphoid organs (2) and much more conspicuously so in solid malignancies. Hypoxia not only affects malignant cells but also stromal components including vascular and immune cells such as tumor-infiltrating lymphocytes (TIL; ref. 3). Although there is extensive knowledge on the effects of tissue hypoxia on vascularization and metabolism in tumors, very little is known about the direct or indirect effects of hypoxia on immune system cells (3).

The heterodimeric hypoxia-inducible transcription factors (HIF $\alpha$ / $\beta$ ) 1, 2, and 3 are central elements in the response to hypoxia (4, 5). In normoxic conditions, their HIF $\alpha$  subunits are rapidly degraded as a result of being poly-ubiquitinated by the Von Hippel-Lindau (VHL) E3 ubiquitin ligase complex (6, 7). When O<sub>2</sub> pressure drops under a certain threshold, prolyl-hydroxylases (PHD) that normally act on HIF-1 $\alpha$

become nonfunctional. In the absence of hydroxylation, HIF $\alpha$  subunits are not amenable to poly-ubiquitination by VHL and thereby are not degraded by the proteasome. As a result, HIF $\alpha$  subunits translocate to the nucleus and dimerize with the constitutively expressed HIF-1 $\beta$  subunit. The spectrum of genes controlled directly (by binding to hypoxia-responding elements in promoters/enhancers) or indirectly (by intermediary genes induced by HIF-1 $\alpha$ / $\beta$ ) is enormous. The goal of the transcriptional hypoxia response is to ensure cell functional survival under hypoxically hostile conditions and to increase vascularization. Once cell normoxia is regained, VHL can act again on HIF $\alpha$  subunits and the response is accordingly repressed.

Our group has recently published that vascular endothelial cells in solid tumors selectively express surface CD137 (4-1BB; ref. 8). Interestingly, the microenvironmental factor driving CD137 expression was found to be hypoxia.

CD137 (4-1BB) is a member of the TNF receptor (TNFR) family (TNFRSF9) originally described on activated T lymphocytes (9). Its transcriptional induction relies mainly on NF- $\kappa$ B and AP-1 (10) as triggered by the TCR-CD3 complex. Once at the cell surface, CD137 provides upon ligation costimulatory signals to T cells (11) and activates natural killer (NK) cell functions (12). Moreover, CD137 is also functionally expressed on dendritic cells (DC; 13) and endothelial cells undergoing inflammation (14) or hypoxia (8). CD137 is stimulated by its only known natural ligand (CD137L, 4-1BBL) whose expression is mainly restricted to the surface of activated antigen-presenting cell (APC; macrophages, DCs, and B cells; ref. 11).

The CD137-CD137L receptor-ligand pair under physiologic conditions is apparently not very important in light of the mild immune phenotypes of CD137<sup>-/-</sup> and CD137L<sup>-/-</sup> mice, which only suffer from a discrete CTL defect in

**Authors' Affiliations:** <sup>1</sup>CIMA and CUN University of Navarra, Pamplona, Navarra; <sup>2</sup>Servicio de Inmunología, Hospital la Princesa, Madrid, Spain; and <sup>3</sup>Bristol-Myers Squibb, Research and Development, Princeton, New Jersey

**Note:** Supplementary data for this article are available at Cancer Discovery Online (<http://cancerdiscovery.aacrjournals.org/>).

**Corresponding Author:** Ignacio Melero, CIMA and Facultad de Medicina Universidad de Navarra, Av. Pio XII, 55, 31008 Pamplona, Navarra 31008, Spain. Phone: 0034948194700; Fax: 011-0034-9481947171; E-mail: imelero@unav.es

doi: 10.1158/2159-8290.CD-11-0314

©2012 American Association for Cancer Research.

antiviral responses (15, 16). Nonetheless, artificial stimulation of CD137 under the overwhelming presence of circulating agonist antibodies provides a strong costimulation *in vivo* (17) that can even revert CTL anergy (18). Importantly, there is plenty of evidence for the efficacy of anti-CD137 monoclonal antibodies (mAb) in the treatment of mice bearing established tumors (17, 19, 20); this is not only achieved by agonist antibodies but also by dimeric RNA aptamers (21) or tumor cells expressing a surface-attached anti-CD137 scFv antibody (22). The main cellular players in those potent antitumoral immune responses seem to be CTLs, but there is also a role for NK cells (12, 18) and DCs (23) at least in some tumor models. This preclinical evidence has led to clinical trials (24) with 2 human mAbs directed against CD137 (BMS-663513 and PF-05082566).

A potential drawback for anti-CD137 mAb is that treatment causes liver inflammation (25, 26). At least in mice, this is dependent on a polyclonal infiltrate dominated by CD3<sup>+</sup>CD8<sup>+</sup>CD11c<sup>-</sup>-activated T cells that mainly occurs in portal spaces. Such an inflammatory response is dose- and target-dependent, and although there are no relevant clinical consequences for mice, it could be otherwise in human patients (24). Therefore, limitation of such liver side effects while keeping therapeutic efficacy would be a remarkable advantage.

In this study, we have documented that CD137 expression is strongly favored in TILs as a result of a HIF-1 $\alpha$ -dependent response to hypoxia. In accordance with the selective CD137 expression in TILs, such lymphocytes are responsive to agonist CD137 mAb. This was exploited by injecting small intratumoral doses of the antibody that were effective without systemically causing liver side effects. From the point of view of therapy, intratumorally delivered low doses of anti-CD137 mAb to target TILs achieve systemic therapeutic effects and act in synergy with the systemic blockade of the PD-1/B7-H1 (PD-L1) pathway. Therefore, hypoxia-mediated upregulation of CD137 on TILs offers the opportunity for confining the therapeutic effects of CD137 agonists to tumors as a safety feature.

## RESULTS

### TILs Express CD137

TILs are a prominent component of tumor stroma. These lymphocytes show features of activation and are known to be enriched for lymphocytes specific for tumor antigens. CT26 is an aggressive transplantable colon carcinoma cell line. CT26-established tumors in syngeneic mice harbor CD4<sup>+</sup> and CD8<sup>+</sup> T cells. To study whether TILs express the CD137 activation marker, single-cell suspensions were prepared from tumors, lymph nodes, and spleens.

As can be seen in Fig. 1A and B, CD137 was minimally expressed by T cells in spleens and lymph nodes of tumor-bearing animals but it was brightly present on CD4<sup>+</sup> and CD8<sup>+</sup> T cells in the tumor compartment. As a control, TILs in CT26-derived tumors grafted onto CD137<sup>-/-</sup> mice (8) showed no evidence of CD137 immunostaining, excluding nonspecific binding of the anti-CD137 antibodies. Figure 1C, representative of a large number of microscopic fields, shows *in situ* immunofluorescence evidence in the tumor

microenvironment for CD4 and CD8 T cells clearly co-expressing CD137.

Among CD4<sup>+</sup> TILs, it was found that CD137 was brightly expressed on the surface of CD4<sup>+</sup>FOXP3<sup>+</sup> regulatory T cells (Treg; Supplementary Fig. S1A). It is of note that CD137 expression was not found on NK cells (CD3<sup>-</sup>DX5<sup>+</sup>) at the tumor, whereas expression on tumor-infiltrating NKT cells (CD3<sup>+</sup>DX5<sup>+</sup>) was found at dim levels (Supplementary Fig. S1B). With regard to other leukocytes infiltrating the tumors, CD137 expression was undetectable on CD19<sup>+</sup> B cells (Supplementary Fig. S2A), F4/80<sup>+</sup> macrophages (Supplementary Fig. S2B), CD11b<sup>+</sup>GR-1<sup>+</sup> myeloid cells (Supplementary Fig. S2C), and CD11c<sup>high</sup> DCs (Supplementary Fig. S2D).

CD137 expression on CD3<sup>+</sup> TILs was not an exclusive feature of CT26-derived tumors as it was also readily observed in transplanted syngenic tumors derived from MC38 colon carcinomas and B16 melanomas (Fig. 2A and B). Indeed, the pattern of selective CD137 expression on T lymphocytes at the tumor, in the absence of CD137 expression on splenocytes or lymph node lymphocytes, was also confirmed in these tumor models. Furthermore, a similar distribution of CD137 was observed in the *Her-2/neu* transgenic female mice bearing spontaneous adenocarcinomas, albeit CD137 expression was dimmer than in transplanted tumors and the number of TILs was much lower (Fig. 2C). In any case, CD137 is expressed on TILs from spontaneous tumors arising in tumor-prone oncogene-transgenic mice.

### Hypoxia Upregulates CD137 Expression on T Cells

The factors upregulating CD137 expression on TILs could be multiple, including the presence of cognate antigen. However, we have reported that hypoxia is a driving factor for ectopic CD137 expression on endothelial cells in tumor blood vessels (8).

We investigated whether hypoxia could be a factor underlying CD137 expression on T cells. First, we found that in tumors in which we detect CD137<sup>+</sup>, TILs are indeed undergoing hypoxia as documented on living mice by sensitive <sup>18</sup>F-MISO positron emission tomographic (PET) imaging based on imidazole chemistry (10). This property applies both to transplanted (CT26, MC38, B16-OVA) and spontaneous tumors (Supplementary Fig. S3A–S3C).

Hypoxia by itself did not upregulate CD137 expression in cultured T lymphocytes in absence of TCR-CD3 triggering (data not shown). However, hypoxia (1% O<sub>2</sub>) clearly upregulated CD137 expression upon T-cell stimulation via CD3/CD28. Indeed, as can be seen in Fig. 3A, suboptimal stimulation using latex microbeads coated with anti-CD3 and anti-CD28 mAb rendered little CD137 surface expression on CD4<sup>+</sup> and CD8<sup>+</sup> spleen T cells. Culture under hypoxic conditions greatly upregulated CD137 surface expression in comparison with normoxic conditions. Moreover, such effects of hypoxia-elicited CD137 upregulation were confirmed at the protein and mRNA level with T-cell receptor (TCR) transgenic T cells stimulated with their cognate peptide antigens (Fig. 3B and C). In fact, OT-1 and OT-2 TCR-transgenic lymphocytes in culture were susceptible to CD137 upregulation upon exposure to hypoxia.



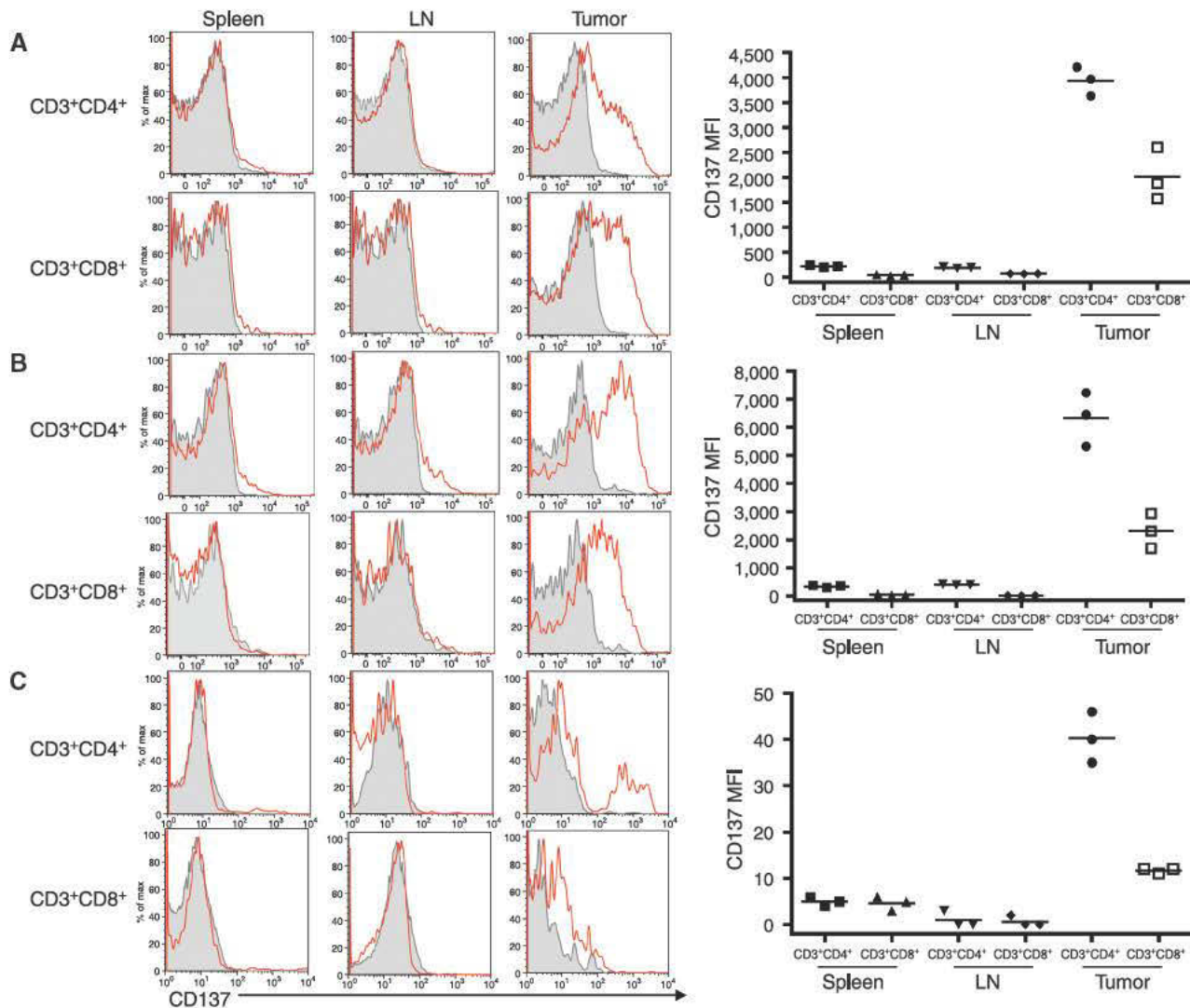


**Figure 2.** Expression of CD137 on TILs is a feature shared by transplantable and spontaneous tumors. **A–C**, experiments as in Fig. 1 with mice bearing established subcutaneous tumors derived from the B16-OVA melanoma and the MC38 colon carcinoma cell lines. Right graphs show a summary of experiments from 3 mice from each tumor type analyzed with a digital FACSCanto. LN, lymph node. **C**, experiments as in Fig. 1 carried out in BALB/c MMTV-*Her2-Neu* transgenic female mice bearing multiple breast carcinomas that were excised and pooled to prepare single-cell suspensions.

To exclude indirect effects mediated by other cell subsets present in the splenocyte cultures, we carried out experiments on CD4 and CD8 immunomagnetically sorted T cells isolated by negative selection. Such experiments rendered comparable results with those carried out with total splenocytes (Supplementary Fig. S4A).

### HIF-1 $\alpha$ Mediates CD137 Expression on T Cells

In response to hypoxia, several cellular changes occur. The main route responding to hypoxia is under the control of the HIF transcription factors. HIF-1 $\alpha$  and HIF-2 are hydroxylated in prolyl residues by specific hydroxylases. The hydroxylated forms are rapidly degraded, whereas the nonhydroxylated forms are stable and exert transcriptional effects following nuclear translocation.

To study whether HIF-1 $\alpha$  responses were involved in CD137 upregulation, first we used a PHD inhibitor [dimethylxylgly-

lycine (DMOG)] and second we carried out experiments with HIF-1 $\alpha$ -deficient T cells.

Figure 4A shows that DMOG-treated OT-1 and OT-2 lymphocytes stimulated by their cognate antigens expressed surface CD137 at a higher intensity. Such increases were comparable with those observed upon culture under hypoxic conditions. Results were consistent with robust inductions of CD137 mRNA (Fig. 4A, bottom).

Treg cells expressed bright intensity of surface CD137 in the cultures placed under normoxia and hypoxia, indicating that there was no need for hypoxia to drive intense CD137 expression in this immunosuppressive subset (Supplementary Fig. S4B).

In humans, we observed that CD4 and CD8 T cells stimulated by plate-bound anti-CD3 mAb and cultured under hypoxia upregulated CD137 more intensely in 48 hours than lymphocytes cultured under normoxic conditions (Supplementary Fig. S5A and S5B). These experiments carried out

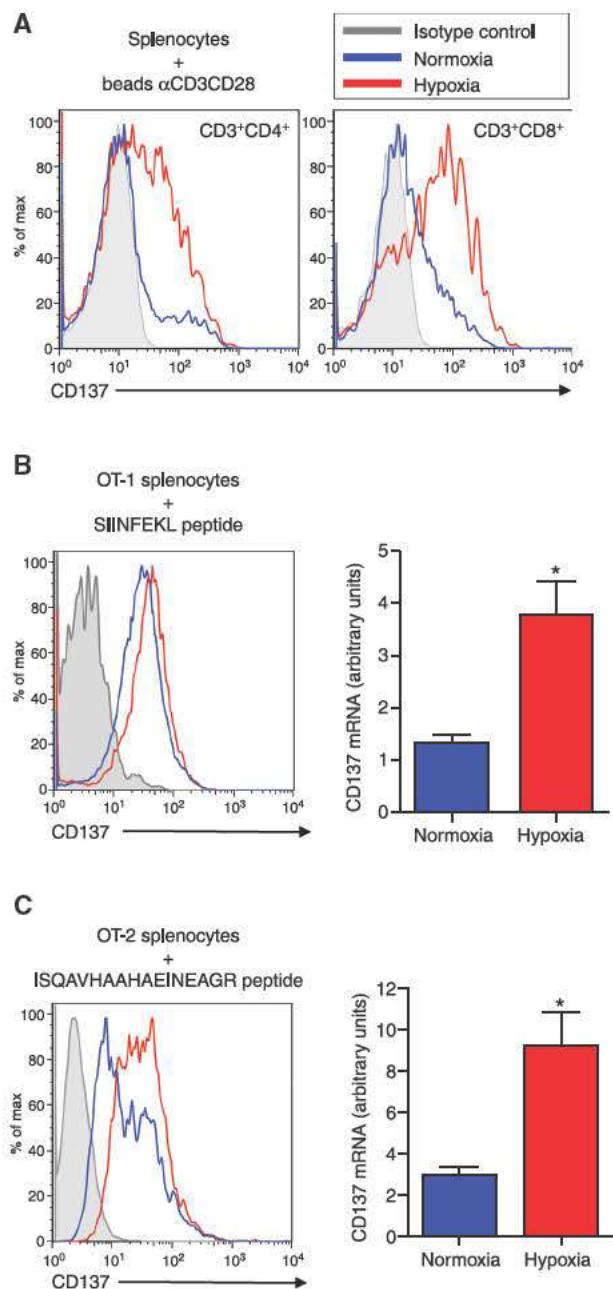


**Figure 3.** Hypoxia upregulates CD137 expression in T lymphocytes undergoing activation. **A**, total splenocytes from C57Bl/6 mice were cultured with latex beads coated with anti-CD3- and anti-CD28-specific mAb at a suboptimal 1:20 bead:cell ratio. Histograms represent CD137 expression in 48-hour cultures analyzed by flow cytometric gating on CD3<sup>+</sup>CD4<sup>+</sup>- or CD3<sup>+</sup>CD8<sup>+</sup>-activated lymphoblasts. CD137-specific stainings were compared with a control isotype-matched antibody tagged with the same fluorochrome (shaded histogram) and are presented in histograms of the indicated line color depending on whether the culture was conducted under normoxia (21% O<sub>2</sub>) or hypoxia (1% O<sub>2</sub>). **B** and **C**, splenocytes from OT1 or OT-2 TCR-transgenic mice were cultured for 24 hours in the presence of the corresponding cognate OVA peptides at 1 μg/mL either under normoxia or hypoxia. CD137 expression was measured by flow cytometry at 24 hours of culture gating on CD8<sup>+</sup> or CD4<sup>+</sup> T cells (left) and by quantitative RT-PCR (right). \*, *P* < 0.05.

with peripheral blood mononuclear cell (PBMC) derived from buffy coats of healthy blood donors showed indications of individual variability in the degree of CD137 upregulation by hypoxia (low vs. high responders in Supplementary Fig. S5A). Similarly, when the cultures on plate-bound anti-CD3 mAbs were treated with DMOG, CD4 and CD8 T cells upregulated surface CD137 more intensely, indicating the involvement of the PHD controlling HIF-1α (Supplementary Fig. S5C).

In a more direct set of experiments, the involvement of HIF-1α was addressed using T cells from mice induced to become deficient in HIF-1α. For this purpose, we used *Hif1α<sup>flxed</sup>-UBC-Cre-ERT2* mice harboring 2 loxP sites flanking the exon 2 of the murine Hif-1α locus, as described previously (27). These mice also express ubiquitously the Cre recombinase fused to a mutated estrogen receptor ligand-binding domain (Cre-ERT2), which remains confined in the cytoplasm until 4-hydroxytamoxifen is administered (28). Therefore, Hif-1α is inactivated after 4-hydroxytamoxifen treatment in *Hif1α<sup>flxed</sup>-UBC-Cre-ERT2* but remains intact in the corresponding control mice *Hif1α<sup>wt</sup>-UBC-Cre-ERT2* or *Hif1α<sup>flxed</sup>* (29). In this study, HIF-1α gene inactivation was induced by intraperitoneal injection of 4-hydroxytamoxifen in mice that carry a *Hif1α<sup>flxed</sup>* allele in homozygosity.

Age-matched *Hif1α<sup>flxed</sup>-UBC-Cre-ERT2* and littermate control mice were treated with 4-hydroxytamoxifen, and 1 week later, splenocytes from these groups were stimulated with anti-CD3 mAb either under normoxic or hypoxic conditions. T cells isolated from 4-hydroxytamoxifen-treated *Hif1α<sup>flxed</sup>-UBC-Cre-ERT2*, but not those isolated from 4HT-treated control mice, drastically reduced their *Hif1α* gene expression (data not shown) and did not upregulate surface CD137 in 48 hours of culture (Fig. 4B). This occurred both on HIF-1α-deficient CD4 and CD8 T cells present in these cultures, whereas control spleen T cells readily upregulated the CD137 molecule under hypoxic conditions as a positive control on both lymphocyte subsets. These differences were also observed by quantitative reverse transcription (RT) PCR at the mRNA level (Fig. 4B, right). However, HIF-1α was not required for expression of CD137 on Treg cells (Supplementary Fig. S4B).

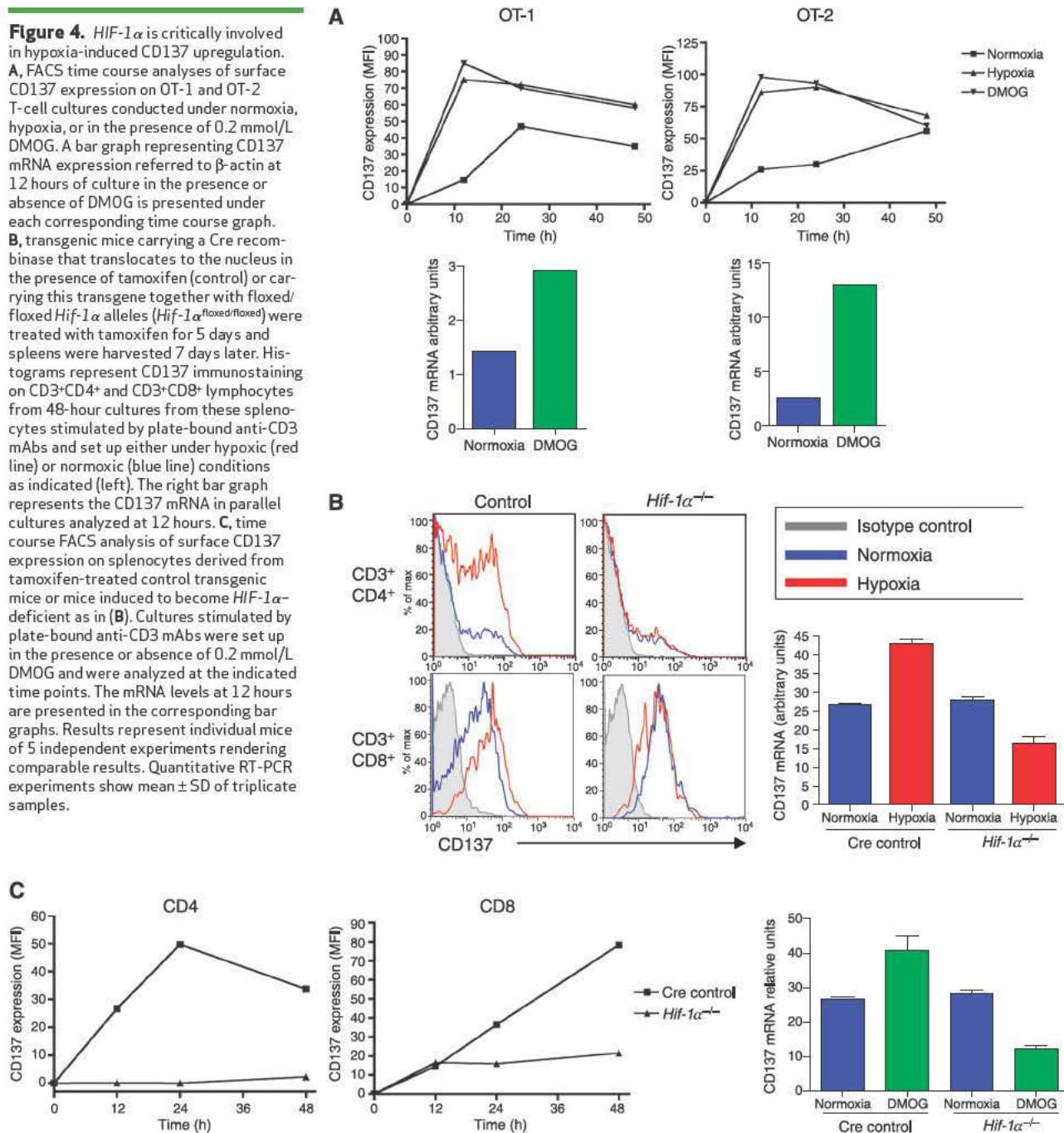
Furthermore, hypoxia and HIF-1α were required for sustained CD137 expression because if hypoxia was only provided during the first 24 hours of culture, the resulting CD4 and CD8 T cells on days 4 and 6 expressed considerably less surface CD137 than those which remained under hypoxia for the duration of the culture (Supplementary Fig. S6A and S6B).

In Fig. 4C, the effect of DMOG on HIF-1α-deficient T cells undergoing CD3-elicited activation is shown at the protein and mRNA levels. Indeed, DMOG did not cause any upregulation of CD137 on HIF-1α-deficient T cells, whereas CD137 was readily induced in T cells from control mice.

### HIF-1α Mediates the Expression of CD137 on TILs

According to these results, TIL expression of CD137 could be at least, in part, an effect of hypoxia as sensed by the HIF-1α system. To further explore this possibility, T cells induced to become HIF-1α-deficient were transferred into mice bearing established MC38-derived subcutaneous tumors. As explained in Fig. 5A, recipient and donor mice were congenic for the CD45.1/CD45.2 allelic polymorphism

**Figure 4.** *HIF-1 $\alpha$*  is critically involved in hypoxia-induced CD137 upregulation. **A**, FACS time course analyses of surface CD137 expression on OT-1 and OT-2 T-cell cultures conducted under normoxia, hypoxia, or in the presence of 0.2 mmol/L DMOG. A bar graph representing CD137 mRNA expression referred to  $\beta$ -actin at 12 hours of culture in the presence or absence of DMOG is presented under each corresponding time course graph. **B**, transgenic mice carrying a Cre recombinase that translocates to the nucleus in the presence of tamoxifen (control) or carrying this transgene together with floxed/floxed *Hif-1 $\alpha$*  alleles (*Hif-1 $\alpha$ <sup>flxed/flxed</sup>*) were treated with tamoxifen for 5 days and spleens were harvested 7 days later. Histograms represent CD137 immunostaining on CD3<sup>+</sup>CD4<sup>+</sup> and CD3<sup>+</sup>CD8<sup>+</sup> lymphocytes from 48-hour cultures from these splenocytes stimulated by plate-bound anti-CD3 mAbs and set up either under hypoxic (red line) or normoxic (blue line) conditions as indicated (left). The right bar graph represents the CD137 mRNA in parallel cultures analyzed at 12 hours. **C**, time course FACS analysis of surface CD137 expression on splenocytes derived from tamoxifen-treated control transgenic mice or mice induced to become *HIF-1 $\alpha$* -deficient as in (B). Cultures stimulated by plate-bound anti-CD3 mAbs were set up in the presence or absence of 0.2 mmol/L DMOG and were analyzed at the indicated time points. The mRNA levels at 12 hours are presented in the corresponding bar graphs. Results represent individual mice of 5 independent experiments rendering comparable results. Quantitative RT-PCR experiments show mean  $\pm$  SD of triplicate samples.



and thereby donor- and recipient-derived TILs could be recognized by specific antibodies upon fluorescence-activated cell sorting (FACS) analyses. With this experimental design, we could compare whether adoptively transferred T cells (CD45.2<sup>+</sup>) upregulated or not CD137 upon infiltration into the tumors in comparison with endogenous T cells (CD45.1<sup>+</sup>). Figure 5A shows that CD3<sup>+</sup> TILs from the *HIF-1 $\alpha$ <sup>-/-</sup>* CD45.2<sup>+</sup> donor did not express surface CD137 whereas CD45.1<sup>+</sup> T cells from the tumor-bearing recipient mice did. As expected, both endogenous and donor T cells were CD137-negative in the spleen (Fig. 5A). The selective

lack of CD137 in *HIF-1 $\alpha$* -deficient TILs applied both to CD4 and CD8 TILs as shown in Fig. 5A.

In these experiments, comparisons were made between adoptively transferred T cells and endogenous T cells. To rule out possible artefacts due to the lack of adoptive transfer of the *HIF-1 $\alpha$* -sufficient lymphocytes in Fig. 5A, experiments were carried out upon adoptive co-transfer of *HIF-1 $\alpha$* -sufficient and -deficient T splenocytes to *Rag1<sup>-/-</sup>* mice bearing MC38 tumors. As can be seen in Fig. 5B, expression of CD137 on TILs was much more intense on CD45.1<sup>+</sup> *HIF-1 $\alpha$* -sufficient T lymphocytes than on CD45.1<sup>-</sup> *HIF-1 $\alpha$* -deficient co-infiltrating lymphocytes.

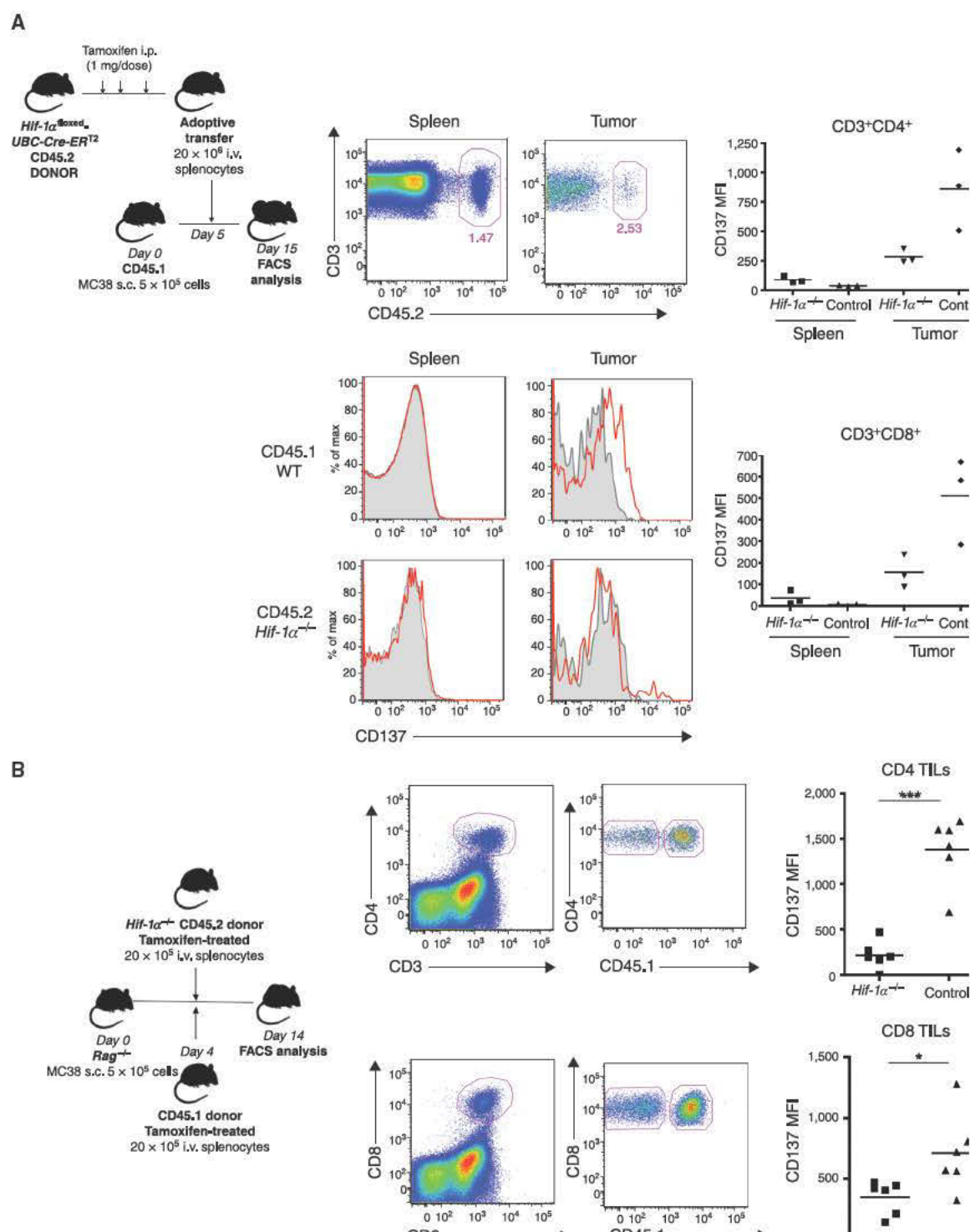


**Figure 5.** TILs upregulate CD137 in an *HIF-1 $\alpha$* -dependent fashion. **A**, *Hif-1 $\alpha$* <sup>flxed</sup>-*UBC-Cre-ERT2* mice homozygous for the CD45.2 allele were induced with tamoxifen for 5 days, checked for loss of HIF-1 $\alpha$ , and 1 week later, their splenocytes were adoptively transferred to congenic C57Bl/6 mice carrying the CD45.1 allele and bearing an established MC38-derived subcutaneous tumor. Ten days later, spleens and tumors were surgically excised and their CD45.1<sup>+</sup> and CD45.2<sup>+</sup> lymphocytes differentially analyzed by FACS. Dot plots show the gating strategy on CD3<sup>+</sup> T cells in the spleen and in the tumor as indicated. Representative histograms on CD45.1- and CD45.2-gated cells in the spleen and in CD3<sup>+</sup> TILs (tumor) are presented. Dot graphs show CD137-specific MFI in CD3<sup>+</sup>CD4<sup>+</sup> and CD3<sup>+</sup>CD8<sup>+</sup> T cells taken from the tumors or the spleens in 3 adoptively transferred mice. WT, wild-type. **B**, experiments as in **(A)** but in this case *Rag*<sup>-/-</sup> mice bearing MC38 tumors for 4 days were adoptively co-transferred with CD45.1 HIF-1 $\alpha$ -sufficient splenocytes from control mice pretreated with tamoxifen and with CD45.2 splenocytes from *Hif-1 $\alpha$* <sup>flxed</sup>-*UBC-Cre-ERT2* pre-induced with 4-hydroxytamoxifen (4-HT). Dot plots show the FACS gating strategy to distinguish CD45.1 positive and negative events between CD4 and CD8 TILs. Dot graphs represent the mean intensity of fluorescence specific for surface anti-CD137 immunostaining on CD4 and CD8 cells from gated CD45.1-positive and -negative TILs.

In conclusion, HIF-1 $\alpha$  in response to hypoxia plays a critical and necessary role in the induction of CD137 expression on TILs.

### Selective Expression of CD137 on TILs Can Be Exploited for Immunotherapy with Anti-CD137 Immunostimulatory mAb

The fact that CD137 expression is largely confined to the tumors could be exploited by intratumoral delivery of the agonist immunotherapeutic mAb. Intratumoral injections of as little as 5  $\mu$ g/dose of 1D8 mAb induced regressions in nearly half of CT26-bearing BALB/c mice treated when the tumors had already reached 5 mm in diameter (day 7).

Systemic treatment with anti-CD137 mAb and anti-B7-H1 (PD-L1) has been described to exert powerful synergistic effects (30). In this CT26 tumor model, repeated 100  $\mu$ g doses of anti-B7-H1 given intraperitoneally (i.p.) attained 5 of 12 complete regressions (Fig. 6A). Importantly, combined treatments of minute doses of anti-CD137 mAb given intratumorally and anti-B7-H1 mAb given systemically achieved complete regressions in 10 of 12 mice (Fig. 6A). These cured mice were immune to a rechallenge with CT26 cells 3 months later (Supplementary Fig. S7) as a result of systemic immune memory.

The effect of B7-H1 blockade is probably due to the fact that grafted CT26 cells forming the tumor mass express B7-H1 on the surface as described in other tumors (31). This is in contrast to the lack of expression on cultured CT26 cells, which can be induced to express B7-H1 by 48-hour culture in the presence of IFN- $\gamma$  (Fig. 6B). In conjunction with the expression of B7-H1 (PD-L1) on the tumor cells, CD4 and CD8 TILs express the checkpoint co-inhibitory molecule PD-1. Hence PD-1<sup>+</sup> TILs should be sensitive to depression by B7-H1 blockade (Fig. 6C). It was also found that PD-1<sup>bright</sup> TILs coincided with CD137<sup>+</sup> TILs. Taken together, these observations probably provide a reason for the synergistic effects of artificial costimulation via CD137 and simultaneous relief from PD-1 inhibition upon blockade of its ligand as previously described by Hirano and colleagues (30).

Importantly, low doses of anti-CD137 mAb achieved remarkable systemic therapeutic effects against concomitant established tumors. This was shown in a bilateral model of CT26-derived tumors transplanted on day 0 to one of the flanks and on day 4 to the opposite side to resemble metastatic disease. On days 7, 9, and 11, the primary lesion was intratumorally treated, whereas the smaller tumor was left untreated. As can be seen in Fig. 6D, 5 of these 7 distant tumor nodules underwent complete rejection, thus indicating the elicitation of concomitant antitumor immunity against tumor nodules that had not been directly treated with the 1D8 anti-CD137 mAb.

Absence of CD137 immunostaining on T cells in tumor-draining lymph nodes was confirmed (Supplementary Fig. S8), further suggesting that the therapeutic costimulatory events were taking place on the TILs. However, upon intratumoral treatment with low doses of 1D8 mAb, there was a clear hyperplasia of tumor-draining lymph nodes that became enlarged 3- to 4-fold over control IgG (Supplementary Fig. S9A).

In addition, the number of TILs increased upon intratumoral treatment with low-dose anti-CD137 mAb (Supplementary Fig. S9A). CD8<sup>+</sup> T cells increased both in terms of percentage and absolute numbers, whereas CD4<sup>+</sup> T cells decreased in absolute and relative numbers (Supplementary Fig. S9B and S9C). As a consequence of a decrease in CD4<sup>+</sup>FOXP3<sup>+</sup> T cells among TILs, a clear increase in the ratio of CD8 T cells/Treg was observed upon 1D8 mAb treatment (Supplementary Fig. S9D). It is of note that following intratumoral treatment, a tendency in the CD8<sup>+</sup> TILs to express higher levels of CD137, Granzyme B, and KLRG-1 was observed (Supplementary Fig. S9E). These results are in line with the observations reported by Curran and colleagues (32) upon systemic treatment with an anti-CD137 antibody. Also, consistent with a more active effector phenotype of such CD8 TILs, these T lymphocytes if restimulated *in vitro* with the AH1 tumor antigen peptide, expressed more IFN- $\gamma$  and TNF- $\alpha$  (Supplementary Fig. S10A–S10C).

### Safer Immunotherapy with Local Low Doses of Anti-CD137 mAb

Agonist anti-CD137 mAbs cause liver inflammation (25). One advantage of giving smaller and more localized doses of anti-CD137 mAb is that the side effects of CD137 known to be dose-dependent would be mitigated. In this regard, Fig. 7 shows that although three 100- $\mu$ g doses of anti-CD137 mAb given i.p. induced mild liver transaminase increases, 5  $\mu$ g given intratumorally 3 times did not cause this side effect (Fig. 7A). This is because CD8 T mononuclear cells do not accumulate forming inflammatory infiltrates in the liver of mice treated with the intratumoral 5- $\mu$ g doses (Fig. 7B–D). Importantly, combinatorial treatments with local anti-CD137 mAb and systemic anti-B7-H1 mAb do not cause liver inflammation (Fig. 7B–D). The idea of conducting intratumoral injections of lower doses of immunostimulatory mAbs had been previously applied successfully by Fransen and colleagues (33) with agonist anti-CD40 mAb. Their strategy also limits systemic toxicity while preserving antitumoral efficacy.

In our case with anti-CD137 mAb, we are exploiting the selective presence of the target for the immunostimulatory antibody at the hypoxic tumor microenvironment to spatially focus the immunotherapeutic effects while avoiding liver toxicity.

## DISCUSSION

Stromal components and malignant cells dialog and mutually change their functional responses. TILs are a prominent feature of malignant tissue whose presence has been correlated with a better survival outcome in various malignant diseases (34, 35). However, TILs are severely restrained in their ability to tackle tumor cells as a result of multifactorial immunosuppressive mechanisms, which are especially intense in the tumor microenvironment (36). Nonetheless, *ex vivo* cultures of TILs to expand and reinvigorate these cells have been used in adoptive cell therapy with reports of impressive objective responses in patients with melanoma (37).

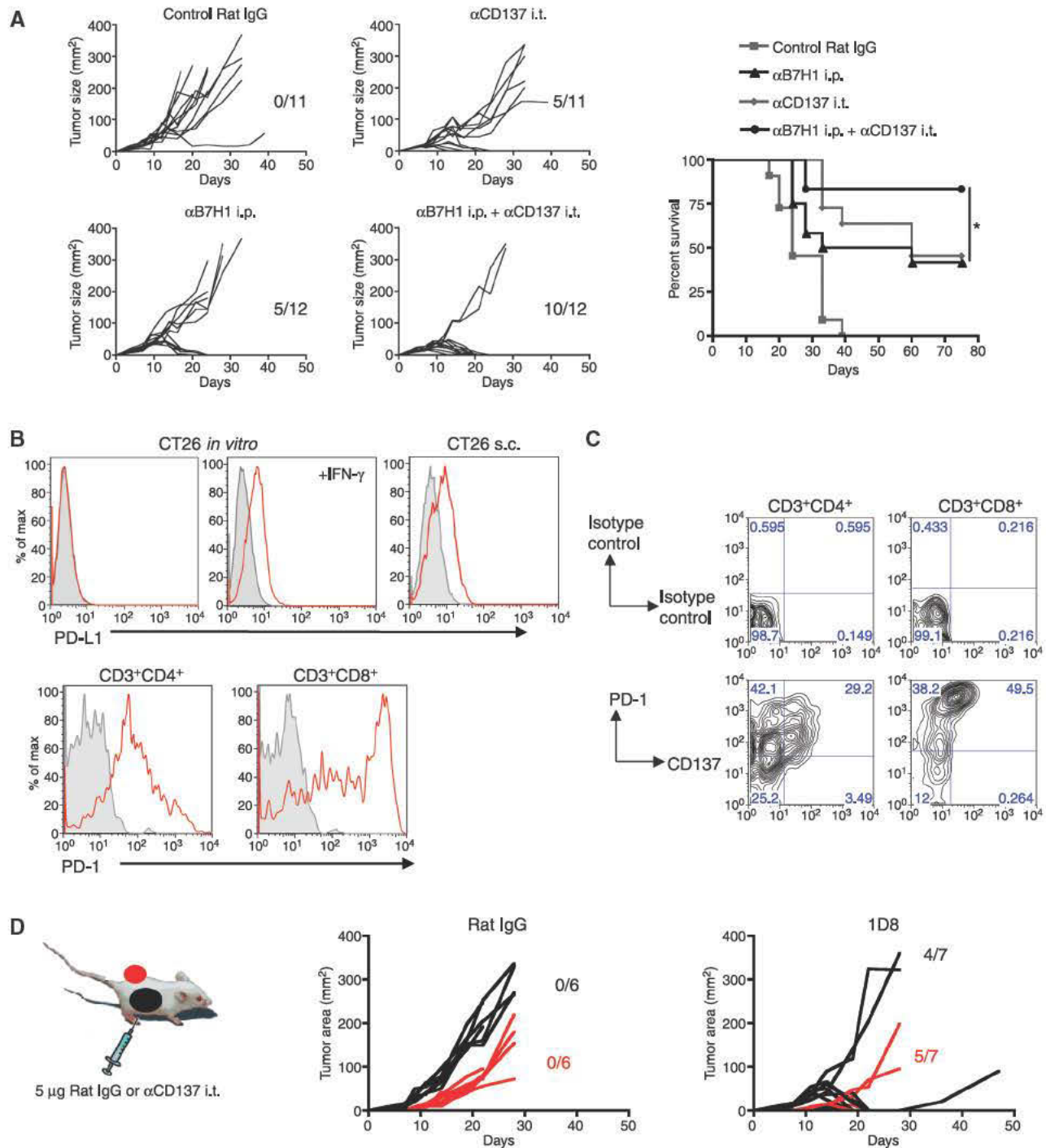


**Figure 6.** Intratumoral injections of small doses of agonist anti-CD137 mAb to directly act on CD137<sup>+</sup> TILs render systemic immunotherapeutic effects that are synergistic with PD-L1 (B7-H1) systemic blockade. **A**, mice bearing subcutaneous CT26 palpable tumors for 7 days were treated intratumorally with three 5- $\mu$ g doses of control rat IgG or anti-CD137 mAb on days 7, 9, and 11 or/and with 3 i.p. doses of 100  $\mu$ g anti-B7-H1 blocking mAb. Individual follow-up of tumor sizes is presented for each experimental group, the fraction of tumor-free mice at the end of the experiment is given in each graph, and the survival curves are presented. i.t., intratumorally. **B**, top, FACS histograms show that CT26 cells do not express B7-H1 in culture but are inducible by culture for 48 hours in the presence of IFN- $\gamma$  or when cells are freshly recovered from grafted tumors in syngeneic mice. Bottom FACS histograms show bright expression of PD-1 on CD3<sup>+</sup>CD4<sup>+</sup> and CD3<sup>+</sup>CD8<sup>+</sup> TILs harvested from CT26 tumors. **C**, dot plots showing CD137 and PD-1 double immunostainings on gated CD8<sup>+</sup> and CD4<sup>+</sup> T cells as indicated. Background immunostainings with isotype-matched control mAb tagged with the same fluorochromes are presented. **D**, BALB/c mice were subcutaneously inoculated with CT26 cells on days 0 and 4 in opposite flanks (black and red as indicated in schematic representation of the experiments). On days 7, 9, and 11, the primary tumor received intratumoral injections of 5  $\mu$ g of 1D8 mAb or control IgG. Graphs represent individual tumor sizes for the primary (black) and secondary (red) tumors. The fraction of mice completely rejecting tumors is provided with the corresponding black and red graphs.

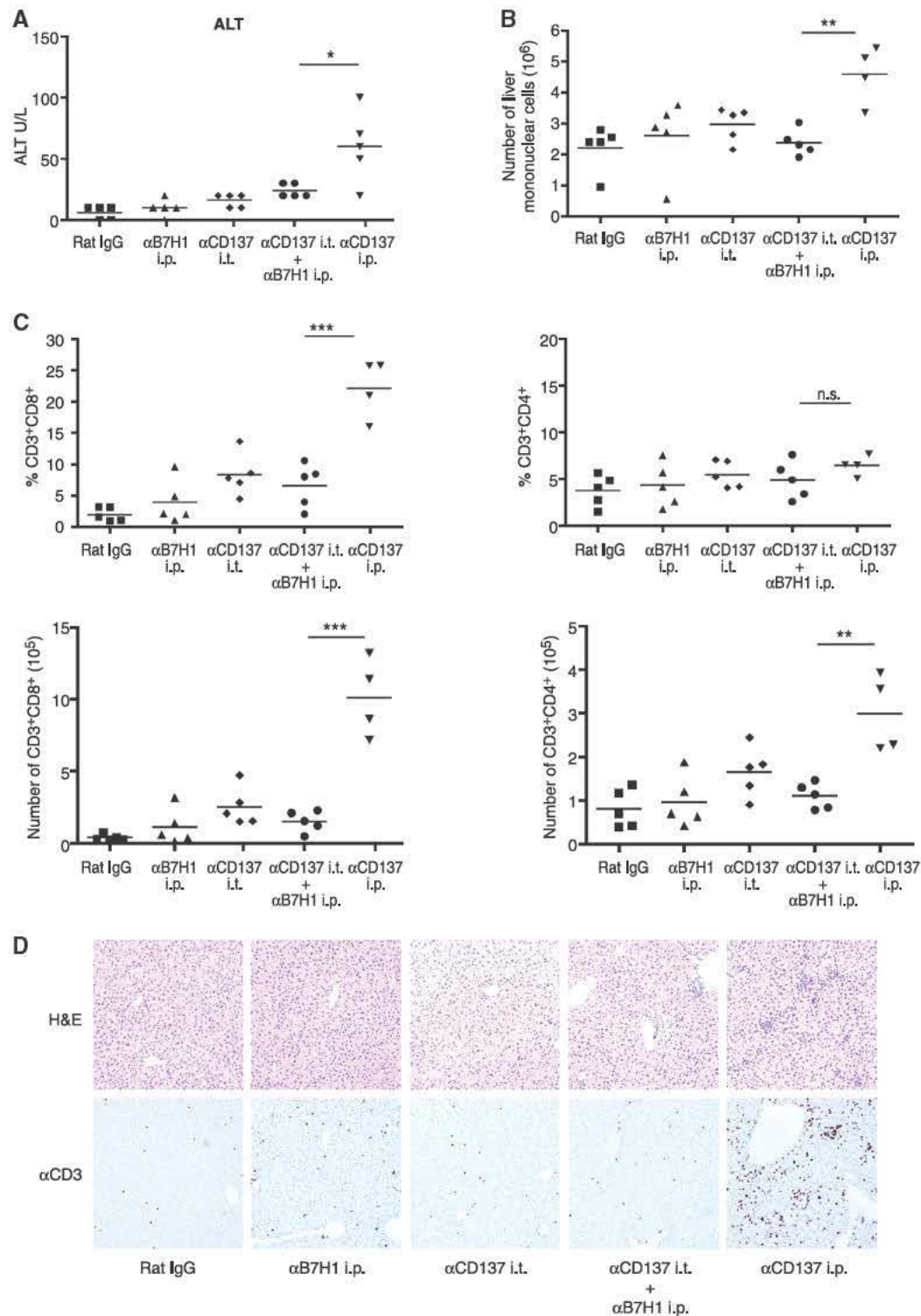


**Figure 7.** Low intratumoral doses of agonist anti-CD137 mAb do not cause liver inflammation. CT26 tumor-bearing mice (5 per group) were treated with the indicated mAbs either intratumorally or intraperitoneally. The i.p. injections consisted of 100  $\mu$ g per dose of mAb given on days 7, 9, 11; and intratumor (i.t.) injections in 5  $\mu$ g per dose given on days 7, 9, and 11. On day 18, mice were sacrificed, blood was drawn, livers were excised, and liver leukocytes were isolated in Percoll gradients. **A**, serum aminolevulinic transaminase serum concentration on day 18. ALT, alanine aminotransferase; \*,  $P < 0.05$ . **B**, the absolute number of mononuclear leukocytes recovered from the liver. \*\*,  $P < 0.01$ . **C**, the percentage (top graphs) and absolute numbers (bottom graphs) of CD4<sup>+</sup> and CD8<sup>+</sup> T cells in the liver as indicated for each group. n.s., not significant; \*\*\*,  $P < 0.001$ . **D**, representative microphotographs ( $\times 200$ ) of hematoxylin and eosin (H&E) stainings and CD3-specific immunohistochemistry of the indicated treatment groups.

Solid tumors are typically compromised in vascularization; as a result, they become hypoxic and respond by producing vascular growth factors to promote angiogenesis. Tumor hypoxia affects both malignant cells and stromal compartments presumably including infiltrating lymphocytes, although there is a conspicuous lack of information in this regard.

Hypoxia has been recently found to induce tumor cell production of a chemokine (CCL28) that attracts Tregs that would locally depress effector cellular immunity (38). However, very little is known about what tumor hypoxia does to tumor-infiltrating T cells directly. Experiments on T-cell cultures set up under hypoxia suggest a decrease in T-cell activation (39, 40), for instance, upon CD3/CD28 stimulation (39). The reasons could involve the HIF response to hypoxia and the effects of released adenosine that acts on inhibitory lymphocyte receptors for this moiety (1).

Moreover, a recent report involves HIF-1 transcription factors in the control of T-helper ( $T_H$ ) 17/Treg balance acting directly on T cells (41). Experiments on conditional HIF-1 $\alpha^{-/-}$  T cells indicate that the HIF-1 response downregulates acquisition of cytokine production and cytolytic activity in CD4 and CD8 T cells (42). Lack of detailed information about T-cell activation under low  $O_2$  tensions is worrying as immune responses in tissues occur at  $\geq 5\%$   $O_2$  (2) and tumors are even more hypoxic, at least in tissue regions located far from blood supply.

We had previously observed that the T-cell activation marker CD137 was upregulated on cultured endothelial cells as a result of hypoxia (8). Anti-CD137 mAb on these CD137 $^+$  endothelial cells elicited proinflammatory changes believed to be involved in the prominent immunotherapeutic effects of anti-CD137 agonist antibodies against tumors because of promoting homing of T lymphocytes to the tumor lesions.

In this study, we found that CD137 is upregulated on TILs but not in secondary lymphoid organs of tumor-bearing mice. Hypoxia was a candidate factor to explain CD137 expression on TILs. Indeed, grafted and spontaneous tumors are clearly hypoxic. However, hypoxia by itself does not induce CD137 on cultured T cells and TCR-CD3 stimulation is required. The striking finding is that CD137 is much more intensely upregulated on T cells undergoing activation when hypoxia is provided. Therefore, we can speculate that both antigen stimulation and hypoxia concurrently coexist in the tumor microenvironment to cooperatively give rise to CD137 expression on TILs. It is intriguing that NK lymphocytes in the tumor that ought to experience the same level of hypoxia do not upregulate CD137. Further studies will address the differential behavior of this lymphocyte subset which also expresses HIF-1 $\alpha$  mRNA.

Hypoxia causes various cellular changes such as induction of functionality of HIF-1 $\alpha$  and HIF-2 transcription factors, generation of free radicals, and adenosine release to the surrounding milieu (1). To ascertain which hypoxia response was involved in CD137 upregulation, we carried out compelling experiments using T cells from HIF-1 $\alpha$ -inducible knockout mice. Such T cells upregulate CD137 much less efficiently when undergoing activation

under hypoxia. Accordingly, experiments in which HIF-1 $\alpha$ -deficient and -sufficient T cells co-infiltrate tumors show that CD137 is selectively expressed on the hypoxia-responsive lymphocytes.

We considered the possibility that CD137 was a direct transcriptional target of HIF-1 $\alpha$ /1 $\beta$ , but detailed bioinformatic analyses of the *cd137* locus did not reveal any interspecies-conserved hypoxia response elements in the noncoding regions 10 kb upstream and downstream of the *cd137* locus including introns (43). Hence, the alternative hypothesis of indirect CD137 enhancing effects mediated by genes upregulated by the transcriptional activity of HIF-1 $\alpha$  is under investigation. In fact, previous reports have revealed a functional interplay of HIF-1 $\alpha$  and NF- $\kappa$ B members (44), whereas canonical NF- $\kappa$ B sites are leading inducers of the CD137 promoter (10). In fact, CD137 upregulation in our experiments seems to take place mainly at the transcriptional level. An antecedent for indirect effects exerted by HIF-1 $\alpha$  in T cells has been recently published by Dang and colleagues (41), who unraveled unexpected functions of HIF-1 $\alpha$  that are critical for the immune system such as protein-to-protein regulation of FOXP3 degradation in CD4 T cells and the control of the expression of secondary transcription factors.

We cannot be sure that cognate antigen and HIF-1 $\alpha$  response are the only factors behind CD137 expression on TILs, but our adoptive transfer experiments with HIF-1 $\alpha$ -deficient T cells clearly indicate that HIF-1 $\alpha$  is a critical factor for CD137 upregulation on TILs. The contribution of hypoxia to CD137 expression on T lymphocytes *in vivo* might extend to other hypoxia situations such as tissues destroyed by infection or atherosclerotic lesions.

The fact that CD137 is a target for a powerful strategy of immunostimulation against cancer makes the observation that TILs are selectively expressing CD137 very appealing. However, the tumor microenvironment is a difficult place for T-cell stimulation because of the abundance of immunoinhibitory factors. Among these suppressive factors, the PD-1/B7-H1 (PD-L1) pathway stands out as hierarchically very important (45, 46). The importance is highlighted by the fact that its blockade is immunotherapeutic in mice and humans (47).

Tregs are perceived also as an important repressor of therapeutic immunity against tumors. We found that CD4 $^+$ FOXP3 $^+$  lymphocytes among TILs express CD137 and would be able to interact with injected anti-CD137 mAb. The effect of CD137 stimulation on Tregs has been reported as dual because despite promoting Treg proliferation, Treg exposure to agonist anti-CD137 mAb weakens the suppressor activities and also desensitizes effector T lymphocytes to the suppressor effects (48). In our study, we confirm bright expression on these suppressive lymphocytes; but in our hands, sensing hypoxia via HIF-1 $\alpha$  is not a prominent driving factor for their expression of CD137.

Agonist anti-CD137 mAbs as monotherapy attain impressive responses against many transplanted tumors, although some of these are resistant including spontaneous breast carcinomas in MMTV-*Neu* mice (20, 49). Although treated mice survive curative anti-CD137 mAb treatments without signs of distress, transient liver inflammation and

myelosuppression have been reported in repeatedly treated animals (26). Fransen and colleagues (33) showed that anti-CD40 mAb at low doses inside tumors can be efficacious without systemic toxicity. We have found that because of the selective presence of CD137 on TILs, the effect of the antibody can be delivered locally without liver inflammation. Importantly, CD137 delivered intratumorally is synergistic with B7-H1 blockade; this synergy had been previously described by Hirano and colleagues (30). Studies in mice chronically infected with LCMV also show synergistic therapeutic effects of anti-CD137 and anti-B7-H1 mAb that correlate with an enhancement of CD8-mediated antiviral immunity (50). Combinatorial treatments with systemic B7-H1 blockade and local agonist anti-CD137 mAbs are highly efficacious. This probably reflects that the very same TILs released from PD-1 inhibition are being provided costimulation via CD137. Importantly, local injection of anti-CD137 mAb attained systemic therapeutic effects against concomitant tumors that are postulated to be mediated by recirculation of the properly stimulated TILs.

Recently, an elegant report from Alizadeh and colleagues (51) has shown that TILs in human lymphomas express surface CD137 and that the amount of CD137 on human pathology specimens of this malignancy correlated favorably with prognosis. Further research should extend these observations to TILs in other human tumors and study a potential correlation with hypoxia.

In summary, CD137 is expressed on TILs because of a response to hypoxia mediated by HIF-1 $\alpha$ . The physiologic reason behind these facts is unknown, but it can be exploited to target CD137 stimulation to where it is most needed, thus limiting systemic side effects. Combinatorial PD-L/B7-H1 (PD-1) pathway blockade and anti-CD137 local stimulation offer many potential clinical advantages, and human immunostimulatory mAbs to all these targets are being tested (24).

## METHODS

### Mice and Cell Lines

BALB/c and C57/BL6 wild-type mice (5 to 6 weeks old) were purchased from Harlan Laboratories. OT-1, OT-2, CD45.1, *Rag*<sup>-/-</sup>, and MMTV-*NeuT* mice (52) were purchased from the Jackson Laboratory and bred in our animal facility under specific pathogen-free conditions. CD137<sup>-/-</sup> mice in pure BALB/c background have been previously described (8).

*Hif-1 $\alpha$* <sup>flxed</sup>-*UBC-Cre-ER*<sup>T2</sup> mice were generated from B6.129-*Hif-1 $\alpha$* <sup>tm3Rsj/J</sup> mice (Jackson Laboratories, stock no. 007561), which harbor 2 *loxP* sites flanking exon 2 of the murine *Hif-1 $\alpha$*  locus. These mice were crossed with *Tg(UBC-Cre/ER*<sup>T2</sup>*)IEjbj* mice (Jackson Laboratories, stock no. 008085) as described above to generate *Hif-1 $\alpha$* <sup>flxed</sup>-*UBC-Cre-ER*<sup>T2</sup> mice and their corresponding controls, *Hif-1 $\alpha$* <sup>wt</sup>-*UBC-Cre-ER*<sup>T2</sup> and *Hif-1 $\alpha$* <sup>flxed</sup> mice. For *Hif-1 $\alpha$*  gene inactivation, *Hif-1 $\alpha$* <sup>flxed</sup>-*UBC-Cre-ER*<sup>T2</sup> and the corresponding control mice (10 to 15 weeks old) were treated with 3 every other day i.p. doses (total of 3 doses) of 1 mg of 4-hydroxytamoxifen (Merck); 7 days after the last dose, the animals were used for experiments. All animal procedures were conducted under Institutional Guidelines that comply with National Laws and Policies (study approval 070-10).

CT26, B16-OVA, and MC38 tumor cell lines were from American Type Culture Collection and the master cell banks authenticated in 2011 by RADIL (Case Number: 6592-2012). Cells were cultured in complete RPMI medium [RPMI-1640 with GlutaMAX (Gibco)

containing 10% heat-inactivated FBS (Sigma-Aldrich), 100 IU/mL penicillin, and 100  $\mu$ g/mL streptomycin (BioWhittaker) and 5  $\times$  10<sup>-5</sup> mol/L 2-mercaptoethanol (Gibco)]. For hypoxic culture conditions, splenocytes were incubated for the indicated times under 1% O<sub>2</sub> atmosphere in a modular incubator chamber (Billups-Rothenberg Inc.) or the H35 Hypoxystation (Don Whitley) for those experiments in which retrieval of part of the cultures from hypoxia was required.

### Human T-cell Experiments

Anonymous buffy coat by-products of blood donations were procured under informed consent of the donors and under approval of the regional committee of ethics of the local government of Navarra. PBMCs were prepared by Ficoll gradients and T cells were stimulated in 6-well plates precoated with 1  $\mu$ g/mL of OKT3 mAb in the same culture medium as in the mouse experiments but without 2-mercaptoethanol. Forty-eight cultures were placed under hypoxia (1% O<sub>2</sub>) or in the presence of 0.2 mmol/L of DMOG when indicated. Retrieved cells were analyzed by flow cytometry upon multicolor immunostaining with fluorochrome anti-CD3, CD4, CD8 (Becton Dickinson) and CD137 (e-bioscience)-specific mAb.

### In Vivo Tumor Growth

A total of 0.5  $\times$  10<sup>6</sup> CT26, MC38, or B16-OVA cells were injected subcutaneously into the flank in 100  $\mu$ L PBS. Mice and tumor size were monitored and mice were sacrificed when tumor size reached 300 mm<sup>2</sup> (53). For some experiments, mice were injected bilaterally in opposite flanks with 0.5  $\times$  10<sup>6</sup> CT26 tumor cells with a delay of 4 days between sites. In those experiments, only the larger primary tumor was injected with the antibody.

### Flow Cytometry, Antibodies, and Tissue Immunofluorescence

For immunofluorescence and flow cytometric analyses of TILs, cleanly excised tumor nodules were placed in Petri dishes, minced finely with a scalpel blade, and incubated for 25 minutes at 37°C in a solution containing Collagenase-D and DNase-I (Roche) in RPMI. The entire material was passed through a 70- $\mu$ m cell strainer (BD Falcon, BD Bioscience) and pressed with a plunger to obtain unicellular cell suspensions. Single-cell suspensions were pretreated with FcR-Block (anti-CD16/32 clone 2.4G2; BD Biosciences-Pharmingen). Afterward, cells were stained with the following antibodies or reagents obtained from BD Pharmingen: CD3, CD4, CD8, CD137, CD49b, CD45.1, PD-1, PD-L1, KLRG-1, F4/80, Gr-1, CD11b, CD11c, Granzyme B, FOXP3, TNF- $\alpha$ , IFN- $\gamma$ , and/or the respective conjugated isotype controls. For TNF- $\alpha$  and IFN- $\gamma$  intracellular staining, tumor mononuclear cells were restimulated with AH1 peptide (SPSYVYHQF 10  $\mu$ g/mL, NeoMPS) for 1 hour and incubated overnight in the presence of brefeldin-A (10  $\mu$ g/mL; Sigma) and then fixed and permeabilized with Fix/perm buffer (eBiosciences) before FACS staining. OT-1 and OT-2 peptides were also from NeoMPS.

FACSCanto II and FACSCalibur (BD Pharmingen) as indicated were used for cell acquisition and data analysis was carried out using FlowJo (TreeStar software).

The hybridomas producing agonistic mouse anti-CD137 (clone 2A) and anti-B7-H1 (PD-L1; clone 10B5) were kindly provided by Dr. Lieping Chen (Yale University, New Haven, CT). Mean fluorescence intensity (MFI) values represent the subtraction of specific versus control MFI. Polyclonal rat IgG with undetectable lipopolysaccharide (LPS; Sigma) was used as control. Mouse anti-CD3/CD28 microbeads were from Dynabeads (Invitrogen). DMOG was purchased from Enzo Life Sciences.

Tissue immunofluorescence staining was conducted on 10- $\mu$ m thick cryosections with the following antibodies: CD4, CD8

(eBiosciences) and goat anti-CD137 (R&D Systems) followed by anti-goat AF488 (Invitrogen) as a secondary antibody. For confocal microscopy, LSM 510 META (Carl Zeiss) equipment was used. The images were analyzed using Zeiss LSM Image Browser software.

### Small-Animal PET Analyses

Tumor hypoxia was measured by PET with the radiotracer fluorine-18-fluoromisonidazole (<sup>18</sup>F-FMISO). On the day of the study, mice were anesthetized with 2% isoflurane in 100% O<sub>2</sub> gas for <sup>18</sup>F-FMISO injection (14.9 ± 4.9 MBq in 100 μL) in the tail vein. Four hours after the tracer injection, mice were placed prone on the PET scanner. A static 30-minute study (sinogram) was acquired using a Mosaic (Philips) small-animal dedicated imaging tomography with 11.9 cm axial field of view (FOV) and 12.8 cm transaxial FOV and a 2-mm resolution. Images were reconstructed using the 3-dimensional (3D) Ramla algorithm (a true 3D reconstruction) with 2 iterations and a relaxation parameter of 0.024 into a 128 × 128 matrix with a 1-mm voxel size applying dead time, decay, random, and scattering corrections.

For the assessment of tumor <sup>18</sup>F-FMISO uptake, all studies were exported and analyzed using the PMOD software (PMOD Technologies Ltd.). Regions of interest were drawn on coronal 1-mm thick small-animal PET images on consecutive slices including the entire tumor. Finally, maximum standardized uptake value (SUV) was calculated for each tumor using the formula  $SUV = [\text{tissue activity concentration (Bq/cm}^3\text{)}/\text{injected dose (Bq)}] \times \text{body weight (g)}$ .

### Molecular Analyses

Total RNA was extracted from lymphocytes using the RNeasy Mini Kit (Qiagen). We treated RNA with DNaseI (Gibco-BRL) before reverse transcription with M-MLV reverse transcriptase (Gibco-BRL) in the presence of RNaseOUT (Gibco-BRL). Real-time PCR was carried out with iQ SYBR green supermix in an iQ5 real-time PCR detection system (Bio-Rad). Copy numbers of CD137 cDNA were quantified by quantitative PCR with primers annealing the mouse CD137 cDNA (forward primer, 5'-AACATCTGCAGAGTGTGTGC-3'; reverse primer, 5'-AGACCTCCGTCTAGAGAGC-3'; product length, 252 bp). Samples were analyzed in triplicate, and data were normalized by comparison with β-actin as an internal control (forward primer, 5'-CGCGTCCACCCGCGAG-3'; reverse primer, 5'-CCTGGTGCCTAGGGCG-3'; product length, 194 bp). The amount of each transcript was expressed according to the formula  $2^{-C_t(\beta\text{-actin}) - \Delta C_t(\text{CD137})}$ , where  $C_t$  is the cycle at which the fluorescence increases appreciably above background fluorescence.

### Adoptive T-cell Transfers

*Hif-1α<sup>floxexd</sup>.UBC-Cre-ER<sup>T2</sup>* or CD45.1 donor mice were treated with tamoxifen. One week later, total splenocytes were inoculated intravenously (10<sup>7</sup> spleen cells per mouse) into CD45.1 or *Rag<sup>-/-</sup>* recipient mice carrying subcutaneous MC38 tumors. Ten days following T-cell transfer, tumors were harvested and analyzed for CD137 expression on CD45.1 versus CD45.2 T cells in a FACSCanto II flow cytometer.

### Statistical Analysis

Prism software (GraphPad Software) was used to determine statistical significance of the differences between groups by applying the unpaired Student *t* tests or 2-way ANOVA tests. *P* values of <0.05 were considered significant.

### Disclosure of Potential Conflicts of Interest

M. Jure-Kunkel is a full-time employee of Bristol-Myers Squibb, I. Melero is a consultant for Bristol-Myers Squibb, Merck-Serono, Pfizer Inc., Miltenyi Biotec, and DIGNA-Biotech and has Ownership

Interest (including patents) in Bristol-Myers Squibb. No potential conflicts of interests were disclosed by the other authors.

### Authors' Contributions

**Conception and design:** A. Palazón, I. Martínez-Forero, J.L. Perez-Gracia, S. Hervás-Stubbs, I. Melero

**Development of methodology:** A. Palazon, A. Morales-Kastresana, C. Alfaro, J.L. Perez-Gracia, S. Hervás-Stubbs, A. Rouzaut, J. Aragonés

**Acquisition of data (provided animals, acquired and managed patients, provided facilities, etc.):** A. Palazón, I. Martínez-Forero, A. Teijeira, I. Peñuelas, A. Rouzaut, M.O. de Landázuri, M. Jure-Kunkel, J. Aragonés

**Analysis and interpretation of data (e.g., statistical analysis, biostatistics, computational analysis):** A. Palazón, I. Martínez-Forero, C. Alfaro, J.L. Perez-Gracia, I. Melero

**Writing, review, and/or revision of the manuscript:** A. Palazon, M.F. de Sanmamed, J.L. Perez-Gracia, M. Jure-Kunkel, I. Melero

**Administrative, technical, or material support (i.e., reporting or organizing data, constructing databases):** A. Palazón, C. Alfaro

**Study supervision:** S. Hervás-Stubbs, I. Melero

**Carried out all experiments:** A. Palazón

### Acknowledgments

The authors acknowledge long-term collaborations on CD137 with Dr. Lieping Chen (Johns Hopkins, Baltimore, MD) and scientific discussion with Dr. Luis del Peso (Universidad Autónoma de Madrid, Madrid, Spain) and Dr. Jesus Prieto (Universidad de Navarra, Navarra, Spain); excellent animal care by Eneko Elizalde and Elena Ciordea; flow cytometric assistance by Dr. Diego Alignani; and English editing by Dr. Paul Miller.

### Grant Support

The financial support was obtained from MEC/MICINN (SAF2005-03131 and SAF2008-03294), Departamento de Educación del Gobierno de Navarra, Departamento de Salud del Gobierno de Navarra; Redes temáticas de investigación cooperativa RETIC (RD06/0020/0065), European commission VII framework program (ENCITE), SUDOE-IMMUNONET, and "UTE for project FIMA". S. Hervás-Stubbs has a Ramon y Cajal contract from MICINN and A. Palazón a scholarship from FIS. A. Morales-Kastresana receives an FPI scholarship from MICINN.

Received November 28, 2011; revised April 23, 2012; accepted April 25, 2012; published OnlineFirst June 19, 2012.

### REFERENCES

1. Sitkovsky MV, Lukashev D, Apasov S, Kojima H, Koshiba M, Caldwell C, et al. Physiological control of immune response and inflammatory tissue damage by hypoxia-inducible factors and adenosine A2A receptors. *Annu Rev Immunol* 2004;22:657-82.
2. Caldwell CC, Kojima H, Lukashev D, Armstrong J, Farber M, Apasov SG, et al. Differential effects of physiologically relevant hypoxic conditions on T lymphocyte development and effector functions. *J Immunol* 2001;167:6140-9.
3. Palazon A, Aragonés J, Morales-Kastresana A, de Landázuri MO, Melero I. Molecular pathways: hypoxia response in immune cells fighting or promoting cancer. *Clin Cancer Res* 2012;18: 1207-13.
4. Semenza GL. Life with oxygen. *Science* 2007;318:62-4.
5. Aragonés J, Fraisl P, Baes M, Carmeliet P. Oxygen sensors at the crossroad of metabolism. *Cell Metab* 2009;9:11-22.

6. Jaakkola P, Mole DR, Tian YM, Wilson MI, Gielbert J, Gaskell SJ, et al. Targeting of HIF- $\alpha$  to the von Hippel-Lindau ubiquitylation complex by O<sub>2</sub>-regulated prolyl hydroxylation. *Science* 2001; 292:468–72.
7. Ivan M, Kondo K, Yang H, Kim W, Valiano J, Ohh M, et al. HIF $\alpha$  targeted for VHL-mediated destruction by proline hydroxylation: implications for O<sub>2</sub> sensing. *Science* 2001;292:464–8.
8. Palazon A, Teixeira A, Martinez-Forero I, Hervas-Stubbs S, Roncal C, Penuelas I, et al. Agonist anti-CD137 mAb act on tumor endothelial cells to enhance recruitment of activated T lymphocytes. *Cancer Res* 2011;71:801–11.
9. Pollok KE, Kim YJ, Zhou Z, Hurtado J, Kim KK, Pickard RT, et al. Inducible T cell antigen 4-1BB. Analysis of expression and function. *J Immunol* 1993;150:771–81.
10. Imam SK. Review of positron emission tomography tracers for imaging of tumor hypoxia. *Cancer Biother Radiopharm* 2010; 25:365–74.
11. Watts TH. TNF/TNFR family members in costimulation of T cell responses. *Annu Rev Immunol* 2005;23:23–68.
12. Melero I, Johnston JV, Shufford WW, Mittler RS, Chen L. NK1.1 cells express 4-1BB (CDw137) costimulatory molecule and are required for tumor immunity elicited by anti-4-1BB monoclonal antibodies. *Cell Immunol* 1998;190:167–72.
13. Choi BK, Kim YH, Kwon PM, Lee SC, Kang SW, Kim MS, et al. 4-1BB functions as a survival factor in dendritic cells. *J Immunol* 2009;182:4107–15.
14. Drenkard D, Becke FM, Langstein J, Spruss T, Kunz-Schughart LA, Tan TE, et al. CD137 is expressed on blood vessel walls at sites of inflammation and enhances monocyte migratory activity. *FASEB J* 2007;21:456–63.
15. Tan JT, Whitmire JK, Ahmed R, Pearson TC, Larsen CP. 4-1BB ligand, a member of the TNF family, is important for the generation of antiviral CD8 T cell responses. *J Immunol* 1999;163:4859–68.
16. Kwon BS, Hurtado JC, Lee ZH, Kwack KB, Seo SK, Choi BK, et al. Immune responses in 4-1BB (CD137)-deficient mice. *J Immunol* 2002;168:5483–90.
17. Melero I, Shufford WW, Newby SA, Aruffo A, Ledbetter JA, Hellstrom KE, et al. Monoclonal antibodies against the 4-1BB T-cell activation molecule eradicate established tumors. *Nat Med* 1997;3:682–5.
18. Wilcox RA, Chapoval AI, Gorski KS, Otsuji M, Shin T, Flies DB, et al. Cutting edge: expression of functional CD137 receptor by dendritic cells. *J Immunol* 2002;168:4262–7.
19. Mittler RS, Foell J, McCausland M, Strahotin S, Niu L, Bapat A, et al. Anti-CD137 antibodies in the treatment of autoimmune disease and cancer. *Immunol Res* 2004;29:197–208.
20. Melero I, Murillo O, Dubrot J, Hervas-Stubbs S, Perez-Gracia JL. Multi-layered action mechanisms of CD137 (4-1BB)-targeted immunotherapies. *Trends Pharmacol Sci* 2008;29:383–90.
21. McNamara JO, Kolonias D, Pastor F, Mittler RS, Chen L, Giangrande PH, et al. Multivalent 4-1BB binding aptamers costimulate CD8<sup>+</sup> T cells and inhibit tumor growth in mice. *J Clin Invest* 2008;118:376–86.
22. Yang Y, Yang S, Ye Z, Jaffar J, Zhou Y, Cutter E, et al. Tumor cells expressing anti-CD137 scFv induce a tumor-destructive environment. *Cancer Res* 2007;67:2339–44.
23. Murillo O, Dubrot J, Palazon A, Arina A, Azpilikueta A, Alfaro C, et al. *In vivo* depletion of DC impairs the anti-tumor effect of agonistic anti-CD137 mAb. *Eur J Immunol* 2009;39:2424–36.
24. Ascierto PA, Simeone E, Sznol M, Fu YX, Melero I. Clinical experiences with anti-CD137 and anti-PD1 therapeutic antibodies. *Semin Oncol* 2010;37:508–16.
25. Dubrot J, Milheiro F, Alfaro C, Palazon A, Martinez-Forero I, Perez-Gracia JL, et al. Treatment with anti-CD137 mAbs causes intense accumulations of liver T cells without selective antitumor immunotherapeutic effects in this organ. *Cancer Immunol Immunother* 2010;59:1223–33.
26. Niu L, Strahotin S, Hewes B, Zhang B, Zhang Y, Archer D, et al. Cytokine-mediated disruption of lymphocyte trafficking, hemopoiesis, and induction of lymphopenia, anemia, and thrombocytopenia in anti-CD137-treated mice. *J Immunol* 2007;178:4194–213.
27. Ryan HE, Lo J, Johnson RS. HIF-1  $\alpha$  is required for solid tumor formation and embryonic vascularization. *EMBO J* 1998; 17:3005–15.
28. Feil R, Wagner J, Metzger D, Chambon P. Regulation of Cre recombinase activity by mutated estrogen receptor ligand-binding domains. *Biochem Biophys Res Commun* 1997;237:752–7.
29. Miro-Murillo M, Elorza A, Soro-Arnaiz I, Albacete-Albacete L, Ordóñez A, Balsa E, et al. Acute Vhl gene inactivation induces cardiac HIF-dependent erythropoietin gene expression. *PLoS One* 2011;6:e22589.
30. Hirano F, Kaneko K, Tamura H, Dong H, Wang S, Ichikawa M, et al. Blockade of B7-H1 and PD-1 by monoclonal antibodies potentiates cancer therapeutic immunity. *Cancer Res* 2005;65:1089–96.
31. Dong H, Strome SE, Salomao DR, Tamura H, Hirano F, Flies DB, et al. Tumor-associated B7-H1 promotes T-cell apoptosis: a potential mechanism of immune evasion. *Nat Med* 2002;8:793–800.
32. Curran MA, Kim M, Montalvo W, Al-Shamkhani A, Allison JP. Combination CTLA-4 blockade and 4-1BB activation enhances tumor rejection by increasing T-cell infiltration, proliferation, and cytokine production. *PLoS One* 2011;6:e19499.
33. Fransen MF, Sluijter M, Morreau H, Arens R, Melief CJ. Local activation of CD8 T cells and systemic tumor eradication without toxicity via slow release and local delivery of agonistic CD40 antibody. *Clin Cancer Res* 2011;17:2270–80.
34. Zhang L, Conejo-Garcia JR, Katsaros D, Gimotty PA, Massobrio M, Regnani G, et al. Intratumoral T cells, recurrence, and survival in epithelial ovarian cancer. *N Engl J Med* 2003;348:203–13.
35. Galon J, Fridman WH, Pages F. The adaptive immunologic microenvironment in colorectal cancer: a novel perspective. *Cancer Res* 2007;67:1883–6.
36. Drake CG, Jaffee E, Pardoll DM. Mechanisms of immune evasion by tumors. *Adv Immunol* 2006;90:51–81.
37. Rosenberg SA. Cell transfer immunotherapy for metastatic solid cancer—what clinicians need to know. *Nat Rev Clin Oncol* 2011;8: 577–85.
38. Facciabene A, Peng X, Hagemann IS, Balint K, Barchetti A, Wang LP, et al. Tumour hypoxia promotes tolerance and angiogenesis via CCL28 and T(reg) cells. *Nature* 2011;475:226–30.
39. Atkuri KR, Herzenberg LA, Niemi AK, Cowan T. Importance of culturing primary lymphocytes at physiological oxygen levels. *Proc Natl Acad Sci U S A* 2007;104:4547–52.
40. Atkuri KR, Herzenberg LA. Culturing at atmospheric oxygen levels impacts lymphocyte function. *Proc Natl Acad Sci U S A* 2005;102: 3756–9.
41. Dang EV, Barbi J, Yang HY, Jinasena D, Yu H, Zheng Y, et al. Control of T(H)17/T(reg) balance by hypoxia-inducible factor 1. *Cell* 2011;146:772–84.
42. Lukashev D, Klebanov B, Kojima H, Grinberg A, Ohta A, Berenfeld L, et al. Cutting edge: hypoxia-inducible factor 1 $\alpha$  and its activation-inducible short isoform I.1 negatively regulate functions of CD4<sup>+</sup> and CD8<sup>+</sup> T lymphocytes. *J Immunol* 2006;177: 4962–5.
43. Ortiz-Barahona A, Villar D, Pescador N, Amigo J, del Peso L. Genome-wide identification of hypoxia-inducible factor binding sites and target genes by a probabilistic model integrating transcription-profiling data and *in silico* binding site prediction. *Nucleic Acids Res* 2010; 38:2332–45.
44. Taylor CT. Interdependent roles for hypoxia inducible factor and nuclear factor-kappaB in hypoxic inflammation. *J Physiol* 2008; 586:4055–9.
45. Sakuishi K, Apetoh L, Sullivan JM, Blazar BR, Kuchroo VK, Anderson AC. Targeting Tim-3 and PD-1 pathways to reverse T cell exhaustion and restore anti-tumor immunity. *J Exp Med* 2011;207: 2187–94.
46. Wang S, Chen L. Immunobiology of cancer therapies targeting CD137 and B7-H1/PD-1 cosignal pathways. *Curr Top Microbiol Immunol* 2011;344:245–67.

47. Brahmer JR, Drake CG, Wollner I, Powderly JD, Picus J, Sharfman WH, et al. Phase I study of single-agent anti-programmed death-1 (MDX-1106) in refractory solid tumors: safety, clinical activity, pharmacodynamics, and immunologic correlates. *J Clin Oncol* 2010; 28:3167-75.
48. So T, Lee SW, Croft M. Immune regulation and control of regulatory T cells by OX40 and 4-1BB. *Cytokine Growth Factor Rev* 2008; 19:253-62.
49. Dubrot J, Palazon A, Alfaro C, Azpilikueta A, Ochoa MC, Rouzaut A, et al. Intratumoral injection of interferon-alpha and systemic delivery of agonist anti-CD137 monoclonal antibodies synergize for immunotherapy. *Int J Cancer* 2011;128:105-18.
50. Vezyz V, Penaloza-Macmaster P, Barber DL, Ha SJ, Konieczny B, Freeman GJ, et al. 4-1BB signaling synergizes with programmed death ligand 1 blockade to augment CD8 T cell responses during chronic viral infection. *J Immunol* 2011;187:1634-42.
51. Alizadeh AA, Gentles AJ, Alencar AJ, Liu CL, Kohrt HE, Houot R, et al. Prediction of survival in diffuse large B-cell lymphoma based on the expression of 2 genes reflecting tumor and microenvironment. *Blood* 2011;118:1350-8.
52. Boggio K, Nicoletti G, Di Carlo E, Cavallo F, Landuzzi L, Melani C, et al. Interleukin 12-mediated prevention of spontaneous mammary adenocarcinomas in two lines of Her-2/neu transgenic mice. *J Exp Med* 1998;188:589-96.
53. Tirapu I, Arina A, Mazzolini G, Duarte M, Alfaro C, Feijoo E, et al. Improving efficacy of interleukin-12-transfected dendritic cells injected into murine colon cancer with anti-CD137 monoclonal antibodies and alloantigens. *Int J Cancer* 2004;110:51-60.

# CANCER DISCOVERY

## The HIF-1 $\alpha$ Hypoxia Response in Tumor-Infiltrating T Lymphocytes Induces Functional CD137 (4-1BB) for Immunotherapy

Asís Palazón, Iván Martínez-Forero, Alvaro Teijeira, et al.

*Cancer Discovery* 2012;2:608-623. Published OnlineFirst June 19, 2012.

**Updated version** Access the most recent version of this article at:  
doi:[10.1158/2159-8290.CD-11-0314](https://doi.org/10.1158/2159-8290.CD-11-0314)

**Supplementary Material** Access the most recent supplemental material at:  
<http://cancerdiscovery.aacrjournals.org/content/suppl/2012/05/14/2159-8290.CD-11-0314.DC1.html>

**Cited articles** This article cites 53 articles, 25 of which you can access for free at:  
<http://cancerdiscovery.aacrjournals.org/content/2/7/608.full.html#ref-list-1>

**Citing articles** This article has been cited by 16 HighWire-hosted articles. Access the articles at:  
<http://cancerdiscovery.aacrjournals.org/content/2/7/608.full.html#related-urls>

**E-mail alerts** [Sign up to receive free email-alerts](#) related to this article or journal.

**Reprints and Subscriptions** To order reprints of this article or to subscribe to the journal, contact the AACR Publications Department at [pubs@aacr.org](mailto:pubs@aacr.org).

**Permissions** To request permission to re-use all or part of this article, contact the AACR Publications Department at [permissions@aacr.org](mailto:permissions@aacr.org).

**ABSTRACT**

The tumor microenvironment of transplanted and spontaneous mouse tumors is profoundly deprived of oxygenation as confirmed by positron emission tomographic (PET) imaging. CD8 and CD4 tumor-infiltrating T lymphocytes (TIL) of transplanted colon carcinomas, melanomas, and spontaneous breast adenocarcinomas are CD137 (4-1BB)-positive, as opposed to their counterparts in tumor-draining lymph nodes and spleen. Expression of CD137 on activated T lymphocytes is markedly enhanced by hypoxia and the prolyl-hydroxylase inhibitor dimethyloxalylglycine (DMOG). Importantly, hypoxia does not upregulate CD137 in hypoxia-inducible factor (HIF)-1 $\alpha$ -knockout T cells, and such HIF-1 $\alpha$ -deficient T cells remain CD137-negative even when becoming TILs, in clear contrast to co-infiltrating and co-transferred HIF-1 $\alpha$ -sufficient T lymphocytes. The fact that CD137 is selectively expressed on TILs was exploited to confine the effects of immunotherapy with agonist anti-CD137 monoclonal antibodies to the tumor tissue. As a result, low-dose intratumoral injections avoid liver inflammation, achieve antitumor systemic effects, and permit synergistic therapeutic effects with PD-L1/B7-H1 blockade.

**SIGNIFICANCE:** CD137 (4-1BB) is an important molecular target to augment antitumor immunity. Hypoxia in the tumor microenvironment as sensed by the HIF-1 $\alpha$  system increases expression of CD137 on tumor-infiltrating lymphocytes that thereby become selectively responsive to the immunotherapeutic effects of anti-CD137 agonist monoclonal antibodies as those used in ongoing clinical trials. *Cancer Discov*; 2(7): 608–23. ©2012 AACR.

**INTRODUCTION**

The study of immune cells in culture is routinely conducted under 21% O<sub>2</sub> concentrations. However, in the tissues where immune responses take place, the concentration of O<sub>2</sub> is much lower (1). This is true in secondary lymphoid organs (2) and much more conspicuously so in solid malignancies. Hypoxia not only affects malignant cells but also stromal components including vascular and immune cells such as tumor-infiltrating lymphocytes (TIL; ref. 3). Although there is extensive knowledge on the effects of tissue hypoxia on vascularization and metabolism in tumors, very little is known about the direct or indirect effects of hypoxia on immune system cells (3).

The heterodimeric hypoxia-inducible transcription factors (HIF $\alpha$ / $\beta$ ) 1, 2, and 3 are central elements in the response to hypoxia (4, 5). In normoxic conditions, their HIF $\alpha$  subunits are rapidly degraded as a result of being poly-ubiquitinated by the Von Hippel-Lindau (VHL) E3 ubiquitin ligase complex (6, 7). When O<sub>2</sub> pressure drops under a certain threshold, prolyl-hydroxylases (PHD) that normally act on HIF-1 $\alpha$

become nonfunctional. In the absence of hydroxylation, HIF $\alpha$  subunits are not amenable to poly-ubiquitination by VHL and thereby are not degraded by the proteasome. As a result, HIF $\alpha$  subunits translocate to the nucleus and dimerize with the constitutively expressed HIF-1 $\beta$  subunit. The spectrum of genes controlled directly (by binding to hypoxia-responding elements in promoters/enhancers) or indirectly (by intermediary genes induced by HIF-1 $\alpha$ / $\beta$ ) is enormous. The goal of the transcriptional hypoxia response is to ensure cell functional survival under hypoxically hostile conditions and to increase vascularization. Once cell normoxia is regained, VHL can act again on HIF $\alpha$  subunits and the response is accordingly repressed.

Our group has recently published that vascular endothelial cells in solid tumors selectively express surface CD137 (4-1BB; ref. 8). Interestingly, the microenvironmental factor driving CD137 expression was found to be hypoxia.

CD137 (4-1BB) is a member of the TNF receptor (TNFR) family (TNFRSF9) originally described on activated T lymphocytes (9). Its transcriptional induction relies mainly on NF- $\kappa$ B and AP-1 (10) as triggered by the TCR-CD3 complex. Once at the cell surface, CD137 provides upon ligation costimulatory signals to T cells (11) and activates natural killer (NK) cell functions (12). Moreover, CD137 is also functionally expressed on dendritic cells (DC; 13) and endothelial cells undergoing inflammation (14) or hypoxia (8). CD137 is stimulated by its only known natural ligand (CD137L, 4-1BBL) whose expression is mainly restricted to the surface of activated antigen-presenting cell (APC; macrophages, DCs, and B cells; ref. 11)

The CD137-CD137L receptor-ligand pair under physiologic conditions is apparently not very important in light of the mild immune phenotypes of CD137<sup>-/-</sup> and CD137L<sup>-/-</sup> mice, which only suffer from a discrete CTL defect in

**Authors' Affiliations:** <sup>1</sup>CIMA and CUN University of Navarra, Pamplona, Navarra; <sup>2</sup>Servicio de Inmunología, Hospital la Princesa, Madrid, Spain; and <sup>3</sup>Bristol-Myers Squibb, Research and Development, Princeton, New Jersey

**Note:** Supplementary data for this article are available at Cancer Discovery Online (<http://cancerdiscovery.aacrjournals.org/>).

**Corresponding Author:** Ignacio Melero, CIMA and Facultad de Medicina Universidad de Navarra, Av. Pio XII, 55, 31008 Pamplona, Navarra 31008, Spain. Phone: 0034948194700; Fax: 011-0034-9481947171; E-mail: imelero@unav.es

doi: 10.1158/2159-8290.CD-11-0314

©2012 American Association for Cancer Research.

antiviral responses (15, 16). Nonetheless, artificial stimulation of CD137 under the overwhelming presence of circulating agonist antibodies provides a strong costimulation *in vivo* (17) that can even revert CTL anergy (18). Importantly, there is plenty of evidence for the efficacy of anti-CD137 monoclonal antibodies (mAb) in the treatment of mice bearing established tumors (17, 19, 20); this is not only achieved by agonist antibodies but also by dimeric RNA aptamers (21) or tumor cells expressing a surface-attached anti-CD137 scFv antibody (22). The main cellular players in those potent antitumoral immune responses seem to be CTLs, but there is also a role for NK cells (12, 18) and DCs (23) at least in some tumor models. This preclinical evidence has led to clinical trials (24) with 2 human mAbs directed against CD137 (BMS-663513 and PF-05082566).

A potential drawback for anti-CD137 mAb is that treatment causes liver inflammation (25, 26). At least in mice, this is dependent on a polyclonal infiltrate dominated by CD3<sup>+</sup>CD8<sup>+</sup>CD11c<sup>-</sup>-activated T cells that mainly occurs in portal spaces. Such an inflammatory response is dose- and target-dependent, and although there are no relevant clinical consequences for mice, it could be otherwise in human patients (24). Therefore, limitation of such liver side effects while keeping therapeutic efficacy would be a remarkable advantage.

In this study, we have documented that CD137 expression is strongly favored in TILs as a result of a HIF-1 $\alpha$ -dependent response to hypoxia. In accordance with the selective CD137 expression in TILs, such lymphocytes are responsive to agonist CD137 mAb. This was exploited by injecting small intratumoral doses of the antibody that were effective without systemically causing liver side effects. From the point of view of therapy, intratumorally delivered low doses of anti-CD137 mAb to target TILs achieve systemic therapeutic effects and act in synergy with the systemic blockade of the PD-1/B7-H1 (PD-L1) pathway. Therefore, hypoxia-mediated upregulation of CD137 on TILs offers the opportunity for confining the therapeutic effects of CD137 agonists to tumors as a safety feature.

## RESULTS

### TILs Express CD137

TILs are a prominent component of tumor stroma. These lymphocytes show features of activation and are known to be enriched for lymphocytes specific for tumor antigens. CT26 is an aggressive transplantable colon carcinoma cell line. CT26-established tumors in syngeneic mice harbor CD4<sup>+</sup> and CD8<sup>+</sup> T cells. To study whether TILs express the CD137 activation marker, single-cell suspensions were prepared from tumors, lymph nodes, and spleens.

As can be seen in Fig. 1A and B, CD137 was minimally expressed by T cells in spleens and lymph nodes of tumor-bearing animals but it was brightly present on CD4<sup>+</sup> and CD8<sup>+</sup> T cells in the tumor compartment. As a control, TILs in CT26-derived tumors grafted onto CD137<sup>-/-</sup> mice (8) showed no evidence of CD137 immunostaining, excluding nonspecific binding of the anti-CD137 antibodies. Figure 1C, representative of a large number of microscopic fields, shows *in situ* immunofluorescence evidence in the tumor

microenvironment for CD4 and CD8 T cells clearly co-expressing CD137.

Among CD4<sup>+</sup> TILs, it was found that CD137 was brightly expressed on the surface of CD4<sup>+</sup>FOXP3<sup>+</sup> regulatory T cells (Treg; Supplementary Fig. S1A). It is of note that CD137 expression was not found on NK cells (CD3<sup>-</sup>DX5<sup>+</sup>) at the tumor, whereas expression on tumor-infiltrating NKT cells (CD3<sup>+</sup>DX5<sup>+</sup>) was found at dim levels (Supplementary Fig. S1B). With regard to other leukocytes infiltrating the tumors, CD137 expression was undetectable on CD19<sup>+</sup> B cells (Supplementary Fig. S2A), F4/80<sup>+</sup> macrophages (Supplementary Fig. S2B), CD11b<sup>+</sup>GR-1<sup>+</sup> myeloid cells (Supplementary Fig. S2C), and CD11c<sup>high</sup> DCs (Supplementary Fig. S2D).

CD137 expression on CD3<sup>+</sup> TILs was not an exclusive feature of CT26-derived tumors as it was also readily observed in transplanted syngenic tumors derived from MC38 colon carcinomas and B16 melanomas (Fig. 2A and B). Indeed, the pattern of selective CD137 expression on T lymphocytes at the tumor, in the absence of CD137 expression on splenocytes or lymph node lymphocytes, was also confirmed in these tumor models. Furthermore, a similar distribution of CD137 was observed in the *Her-2/neu* transgenic female mice bearing spontaneous adenocarcinomas, albeit CD137 expression was dimmer than in transplanted tumors and the number of TILs was much lower (Fig. 2C). In any case, CD137 is expressed on TILs from spontaneous tumors arising in tumor-prone oncogene-transgenic mice.

### Hypoxia Upregulates CD137 Expression on T Cells

The factors upregulating CD137 expression on TILs could be multiple, including the presence of cognate antigen. However, we have reported that hypoxia is a driving factor for ectopic CD137 expression on endothelial cells in tumor blood vessels (8).

We investigated whether hypoxia could be a factor underlying CD137 expression on T cells. First, we found that in tumors in which we detect CD137<sup>+</sup>, TILs are indeed undergoing hypoxia as documented on living mice by sensitive <sup>18</sup>F-MISO positron emission tomographic (PET) imaging based on imidazole chemistry (10). This property applies both to transplanted (CT26, MC38, B16-OVA) and spontaneous tumors (Supplementary Fig. S3A–S3C).

Hypoxia by itself did not upregulate CD137 expression in cultured T lymphocytes in absence of TCR-CD3 triggering (data not shown). However, hypoxia (1% O<sub>2</sub>) clearly upregulated CD137 expression upon T-cell stimulation via CD3/CD28. Indeed, as can be seen in Fig. 3A, suboptimal stimulation using latex microbeads coated with anti-CD3 and anti-CD28 mAb rendered little CD137 surface expression on CD4<sup>+</sup> and CD8<sup>+</sup> spleen T cells. Culture under hypoxic conditions greatly upregulated CD137 surface expression in comparison with normoxic conditions. Moreover, such effects of hypoxia-elicited CD137 upregulation were confirmed at the protein and mRNA level with T-cell receptor (TCR) transgenic T cells stimulated with their cognate peptide antigens (Fig. 3B and C). In fact, OT-1 and OT-2 TCR-transgenic lymphocytes in culture were susceptible to CD137 upregulation upon exposure to hypoxia.

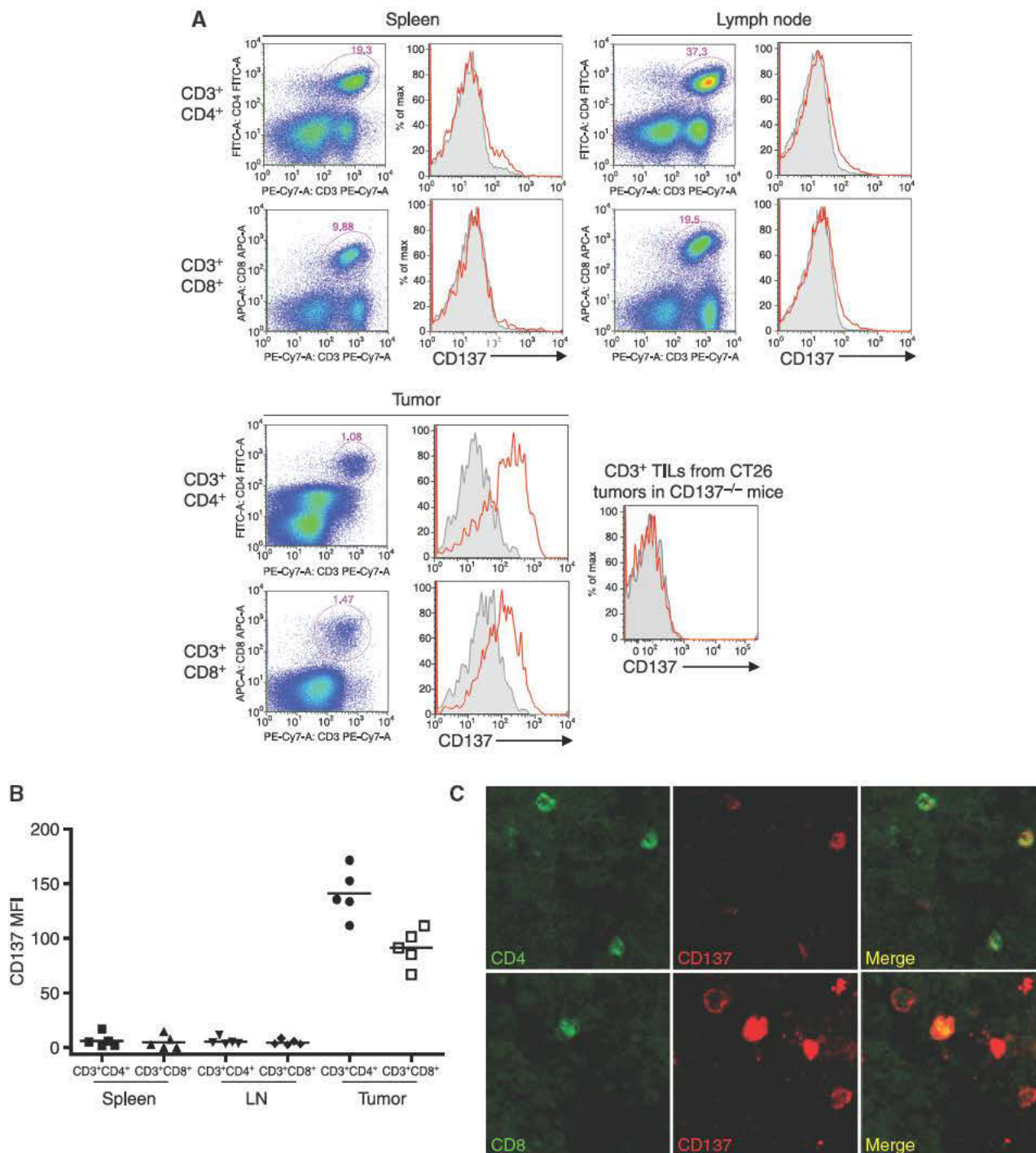


**Figure 1.** CD4<sup>+</sup> and CD8<sup>+</sup> TILs express surface CD137. BALB/c mice bearing CT26-derived subcutaneous tumors for 12 to 14 days were euthanized to prepare single-cell suspensions from tumor nodules, spleens, and lymph nodes. **A**, FACS analysis of CD137 expression on gated CD4 or CD8 T cells from spleen, lymph node, or tumor tissue as indicated. Tinted histograms represent isotype-matched control antibodies and open histograms CD137-specific surface staining from a representative case acquired with an analogic FACSCalibur. As a control to rule out unspecific immunostaining on CD3<sup>+</sup> TILs, TILs from CT26-derived tumors grafted onto CD137<sup>-/-</sup> mice were not stained by the anti-CD137 mAbs used for detection. **B**, summary of data of 5 mice. LN, lymph node. **C**, double immunofluorescence for CD137 and either CD4 or CD8 TILs on CT26 tumor tissue sections. Data are representative of at least 15 microscopic fields in 3 different sections from 3 independent tumors.

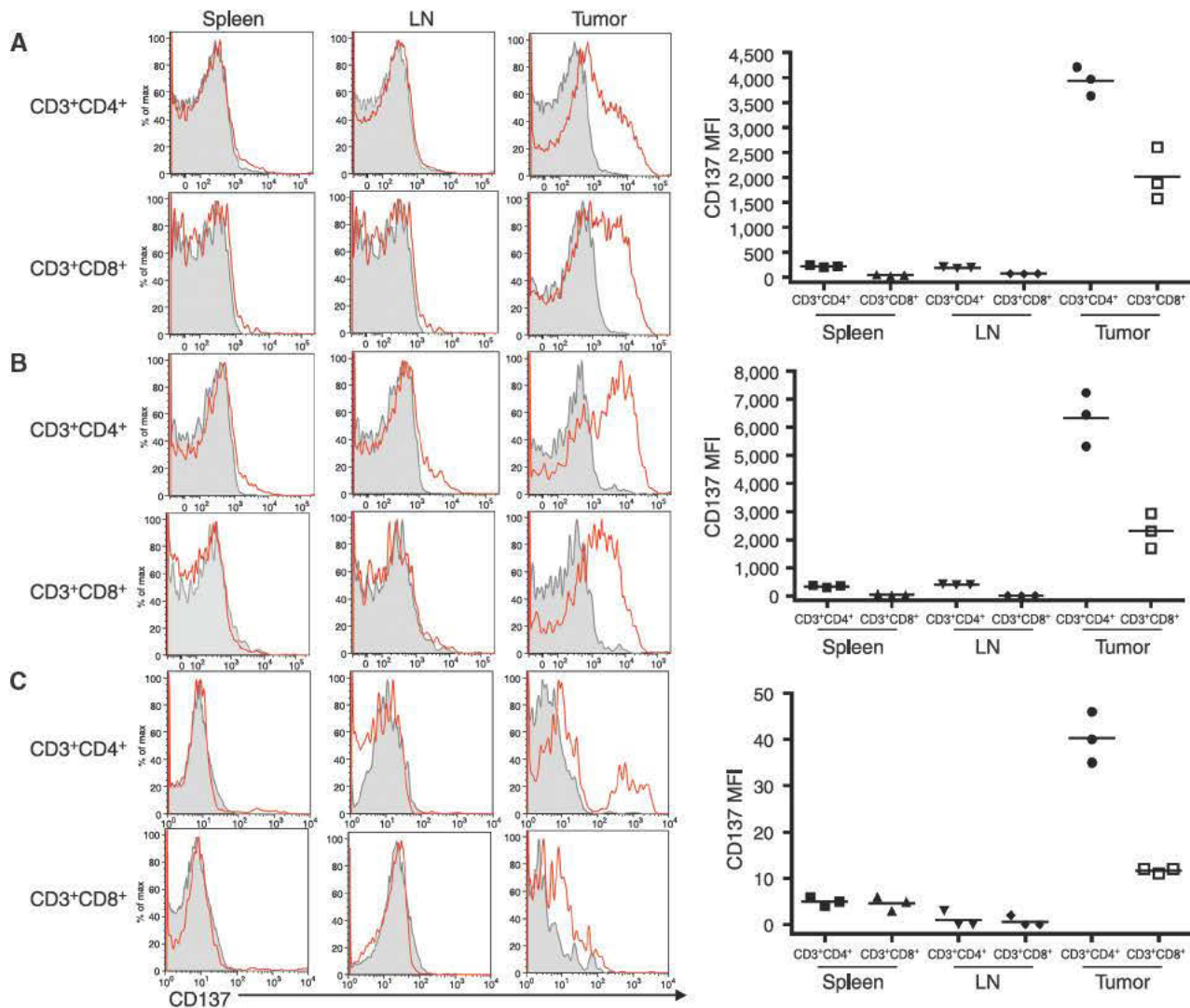


**Figure 2.** Expression of CD137 on TILs is a feature shared by transplantable and spontaneous tumors. **A–C**, experiments as in Fig. 1 with mice bearing established subcutaneous tumors derived from the B16-OVA melanoma and the MC38 colon carcinoma cell lines. Right graphs show a summary of experiments from 3 mice from each tumor type analyzed with a digital FACSCanto. LN, lymph node. **C**, experiments as in Fig. 1 carried out in BALB/c MMTV-*Her2-Neu* transgenic female mice bearing multiple breast carcinomas that were excised and pooled to prepare single-cell suspensions.

To exclude indirect effects mediated by other cell subsets present in the splenocyte cultures, we carried out experiments on CD4 and CD8 immunomagnetically sorted T cells isolated by negative selection. Such experiments rendered comparable results with those carried out with total splenocytes (Supplementary Fig. S4A).

### HIF-1 $\alpha$ Mediates CD137 Expression on T Cells

In response to hypoxia, several cellular changes occur. The main route responding to hypoxia is under the control of the HIF transcription factors. HIF-1 $\alpha$  and HIF-2 are hydroxylated in prolyl residues by specific hydroxylases. The hydroxylated forms are rapidly degraded, whereas the nonhydroxylated forms are stable and exert transcriptional effects following nuclear translocation.

To study whether HIF-1 $\alpha$  responses were involved in CD137 upregulation, first we used a PHD inhibitor [dimethylxalylg-

lycine (DMOG)] and second we carried out experiments with HIF-1 $\alpha$ -deficient T cells.

Figure 4A shows that DMOG-treated OT-1 and OT-2 lymphocytes stimulated by their cognate antigens expressed surface CD137 at a higher intensity. Such increases were comparable with those observed upon culture under hypoxic conditions. Results were consistent with robust inductions of CD137 mRNA (Fig. 4A, bottom).

Treg cells expressed bright intensity of surface CD137 in the cultures placed under normoxia and hypoxia, indicating that there was no need for hypoxia to drive intense CD137 expression in this immunosuppressive subset (Supplementary Fig. S4B).

In humans, we observed that CD4 and CD8 T cells stimulated by plate-bound anti-CD3 mAb and cultured under hypoxia upregulated CD137 more intensely in 48 hours than lymphocytes cultured under normoxic conditions (Supplementary Fig. S5A and S5B). These experiments carried out

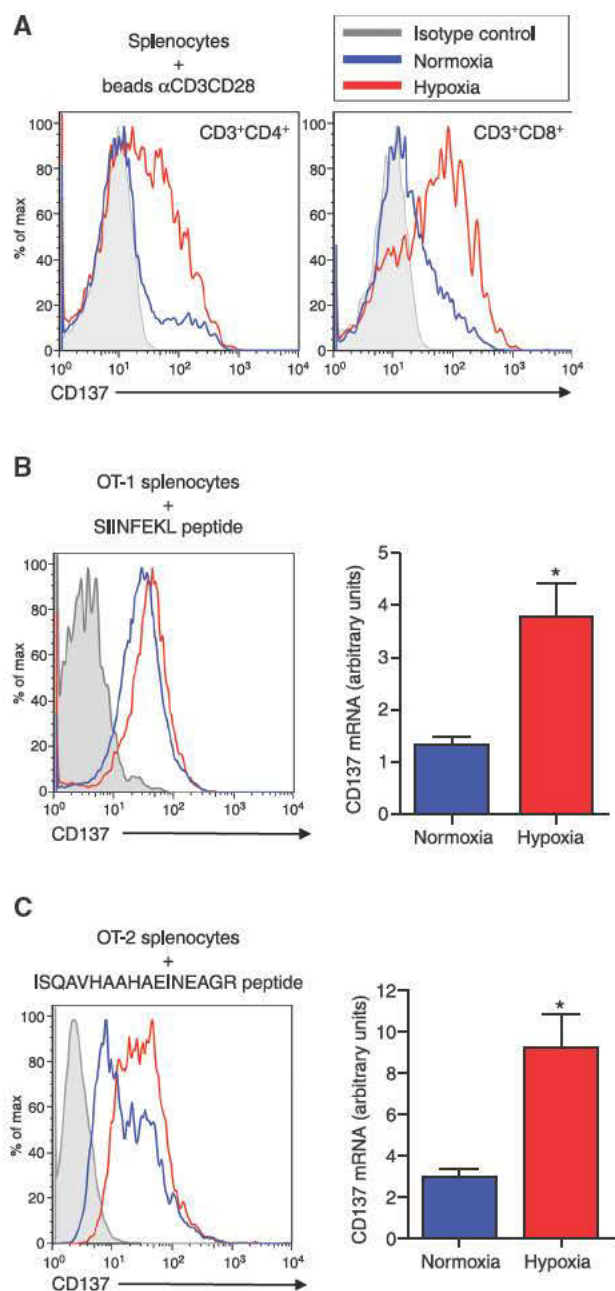


**Figure 3.** Hypoxia upregulates CD137 expression in T lymphocytes undergoing activation. **A**, total splenocytes from C57Bl/6 mice were cultured with latex beads coated with anti-CD3- and anti-CD28-specific mAb at a suboptimal 1:20 bead:cell ratio. Histograms represent CD137 expression in 48-hour cultures analyzed by flow cytometric gating on CD3<sup>+</sup>CD4<sup>+</sup>- or CD3<sup>+</sup>CD8<sup>+</sup>-activated lymphoblasts. CD137-specific stainings were compared with a control isotype-matched antibody tagged with the same fluorochrome (shaded histogram) and are presented in histograms of the indicated line color depending on whether the culture was conducted under normoxia (21% O<sub>2</sub>) or hypoxia (1% O<sub>2</sub>). **B** and **C**, splenocytes from OT1 or OT-2 TCR-transgenic mice were cultured for 24 hours in the presence of the corresponding cognate OVA peptides at 1 μg/mL either under normoxia or hypoxia. CD137 expression was measured by flow cytometry at 24 hours of culture gating on CD8<sup>+</sup> or CD4<sup>+</sup> T cells (left) and by quantitative RT-PCR (right). \*, *P* < 0.05.

with peripheral blood mononuclear cell (PBMC) derived from buffy coats of healthy blood donors showed indications of individual variability in the degree of CD137 upregulation by hypoxia (low vs. high responders in Supplementary Fig. S5A). Similarly, when the cultures on plate-bound anti-CD3 mAbs were treated with DMOG, CD4 and CD8 T cells upregulated surface CD137 more intensely, indicating the involvement of the PHD controlling HIF-1 $\alpha$  (Supplementary Fig. S5C).

In a more direct set of experiments, the involvement of HIF-1 $\alpha$  was addressed using T cells from mice induced to become deficient in HIF-1 $\alpha$ . For this purpose, we used *Hif1 $\alpha$ <sup>flxed</sup>-UBC-Cre-ERT<sup>2</sup>* mice harboring 2 loxP sites flanking the exon 2 of the murine Hif-1 $\alpha$  locus, as described previously (27). These mice also express ubiquitously the Cre recombinase fused to a mutated estrogen receptor ligand-binding domain (Cre-ERT2), which remains confined in the cytoplasm until 4-hydroxytamoxifen is administered (28). Therefore, Hif-1 $\alpha$  is inactivated after 4-hydroxytamoxifen treatment in *Hif1 $\alpha$ <sup>flxed</sup>-UBC-Cre-ERT<sup>2</sup>* but remains intact in the corresponding control mice *Hif1 $\alpha$ <sup>wt</sup>-UBC-Cre-ERT<sup>2</sup>* or *Hif1 $\alpha$ <sup>flxed</sup>* (29). In this study, HIF-1 $\alpha$  gene inactivation was induced by intraperitoneal injection of 4-hydroxytamoxifen in mice that carry a *Hif1 $\alpha$ <sup>flxed</sup>* allele in homozygosity.

Age-matched *Hif1 $\alpha$ <sup>flxed</sup>-UBC-Cre-ERT<sup>2</sup>* and littermate control mice were treated with 4-hydroxytamoxifen, and 1 week later, splenocytes from these groups were stimulated with anti-CD3 mAb either under normoxic or hypoxic conditions. T cells isolated from 4-hydroxytamoxifen-treated *Hif1 $\alpha$ <sup>flxed</sup>-UBC-Cre-ERT<sup>2</sup>*, but not those isolated from 4HT-treated control mice, drastically reduced their *Hif1 $\alpha$*  gene expression (data not shown) and did not upregulate surface CD137 in 48 hours of culture (Fig. 4B). This occurred both on HIF-1 $\alpha$ -deficient CD4 and CD8 T cells present in these cultures, whereas control spleen T cells readily upregulated the CD137 molecule under hypoxic conditions as a positive control on both lymphocyte subsets. These differences were also observed by quantitative reverse transcription (RT) PCR at the mRNA level (Fig. 4B, right). However, HIF-1 $\alpha$  was not required for expression of CD137 on Treg cells (Supplementary Fig. S4B).

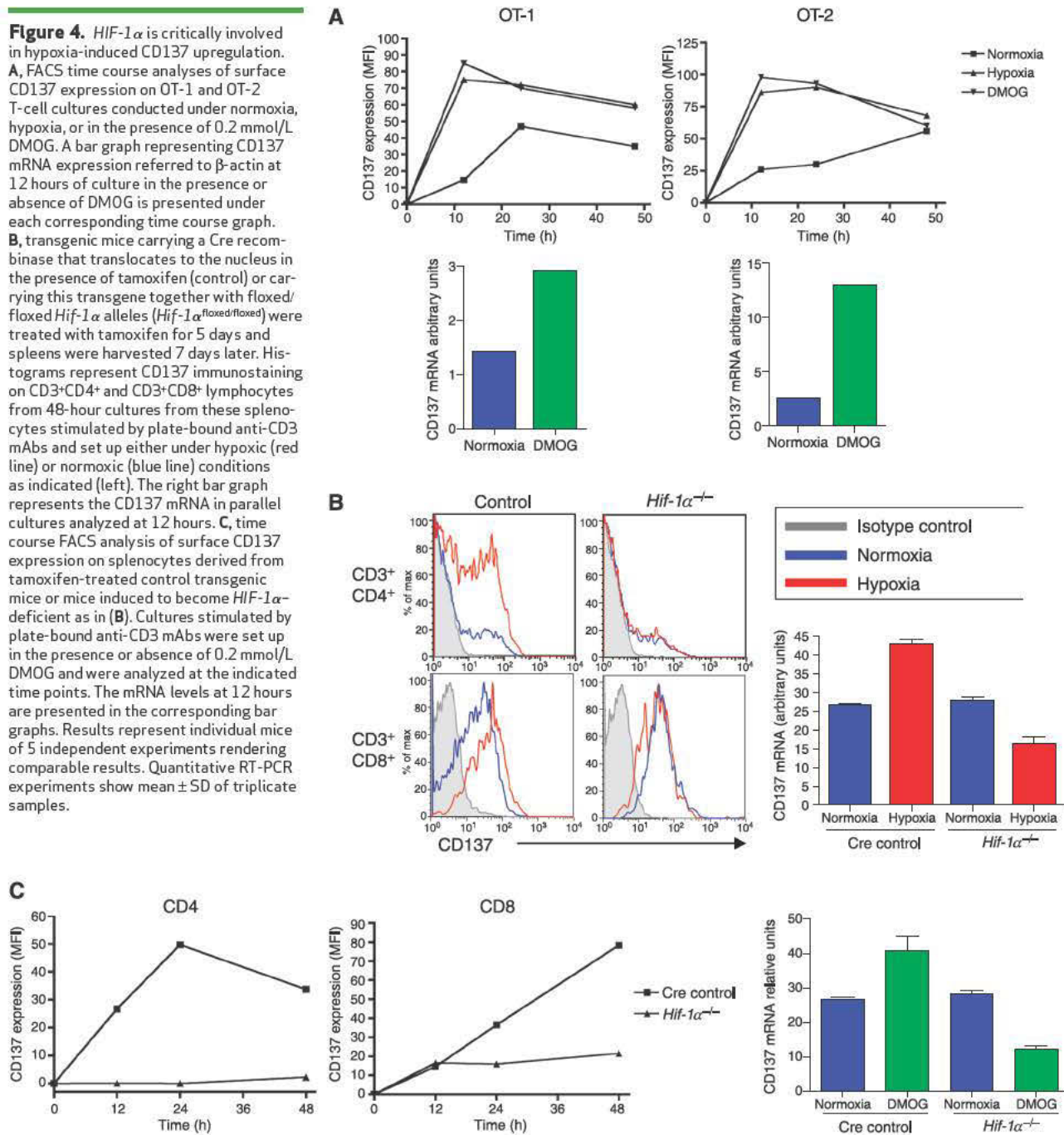
Furthermore, hypoxia and HIF-1 $\alpha$  were required for sustained CD137 expression because if hypoxia was only provided during the first 24 hours of culture, the resulting CD4 and CD8 T cells on days 4 and 6 expressed considerably less surface CD137 than those which remained under hypoxia for the duration of the culture (Supplementary Fig. S6A and S6B).

In Fig. 4C, the effect of DMOG on HIF-1 $\alpha$ -deficient T cells undergoing CD3-elicited activation is shown at the protein and mRNA levels. Indeed, DMOG did not cause any upregulation of CD137 on HIF-1 $\alpha$ -deficient T cells, whereas CD137 was readily induced in T cells from control mice.

### HIF-1 $\alpha$ Mediates the Expression of CD137 on TILs

According to these results, TIL expression of CD137 could be at least, in part, an effect of hypoxia as sensed by the HIF-1 $\alpha$  system. To further explore this possibility, T cells induced to become HIF-1 $\alpha$ -deficient were transferred into mice bearing established MC38-derived subcutaneous tumors. As explained in Fig. 5A, recipient and donor mice were congenic for the CD45.1/CD45.2 allelic polymorphism

**Figure 4.** *HIF-1 $\alpha$*  is critically involved in hypoxia-induced CD137 upregulation. **A**, FACS time course analyses of surface CD137 expression on OT-1 and OT-2 T-cell cultures conducted under normoxia, hypoxia, or in the presence of 0.2 mmol/L DMOG. A bar graph representing CD137 mRNA expression referred to  $\beta$ -actin at 12 hours of culture in the presence or absence of DMOG is presented under each corresponding time course graph. **B**, transgenic mice carrying a Cre recombinase that translocates to the nucleus in the presence of tamoxifen (control) or carrying this transgene together with floxed/floxed *Hif-1 $\alpha$*  alleles (*Hif-1 $\alpha$ <sup>flxed/flxed</sup>*) were treated with tamoxifen for 5 days and spleens were harvested 7 days later. Histograms represent CD137 immunostaining on CD3<sup>+</sup>CD4<sup>+</sup> and CD3<sup>+</sup>CD8<sup>+</sup> lymphocytes from 48-hour cultures from these splenocytes stimulated by plate-bound anti-CD3 mAbs and set up either under hypoxic (red line) or normoxic (blue line) conditions as indicated (left). The right bar graph represents the CD137 mRNA in parallel cultures analyzed at 12 hours. **C**, time course FACS analysis of surface CD137 expression on splenocytes derived from tamoxifen-treated control transgenic mice or mice induced to become *HIF-1 $\alpha$* -deficient as in (B). Cultures stimulated by plate-bound anti-CD3 mAbs were set up in the presence or absence of 0.2 mmol/L DMOG and were analyzed at the indicated time points. The mRNA levels at 12 hours are presented in the corresponding bar graphs. Results represent individual mice of 5 independent experiments rendering comparable results. Quantitative RT-PCR experiments show mean  $\pm$  SD of triplicate samples.



and thereby donor- and recipient-derived TILs could be recognized by specific antibodies upon fluorescence-activated cell sorting (FACS) analyses. With this experimental design, we could compare whether adoptively transferred T cells (CD45.2<sup>+</sup>) upregulated or not CD137 upon infiltration into the tumors in comparison with endogenous T cells (CD45.1<sup>+</sup>). Figure 5A shows that CD3<sup>+</sup> TILs from the *HIF-1 $\alpha$ <sup>-/-</sup>* CD45.2<sup>+</sup> donor did not express surface CD137 whereas CD45.1<sup>+</sup> T cells from the tumor-bearing recipient mice did. As expected, both endogenous and donor T cells were CD137-negative in the spleen (Fig. 5A). The selective

lack of CD137 in *HIF-1 $\alpha$* -deficient TILs applied both to CD4 and CD8 TILs as shown in Fig. 5A.

In these experiments, comparisons were made between adoptively transferred T cells and endogenous T cells. To rule out possible artefacts due to the lack of adoptive transfer of the *HIF-1 $\alpha$* -sufficient lymphocytes in Fig. 5A, experiments were carried out upon adoptive co-transfer of *HIF-1 $\alpha$* -sufficient and -deficient T splenocytes to *Rag1<sup>-/-</sup>* mice bearing MC38 tumors. As can be seen in Fig. 5B, expression of CD137 on TILs was much more intense on CD45.1<sup>+</sup> *HIF-1 $\alpha$* -sufficient T lymphocytes than on CD45.1<sup>-</sup> *HIF-1 $\alpha$* -deficient co-infiltrating lymphocytes.

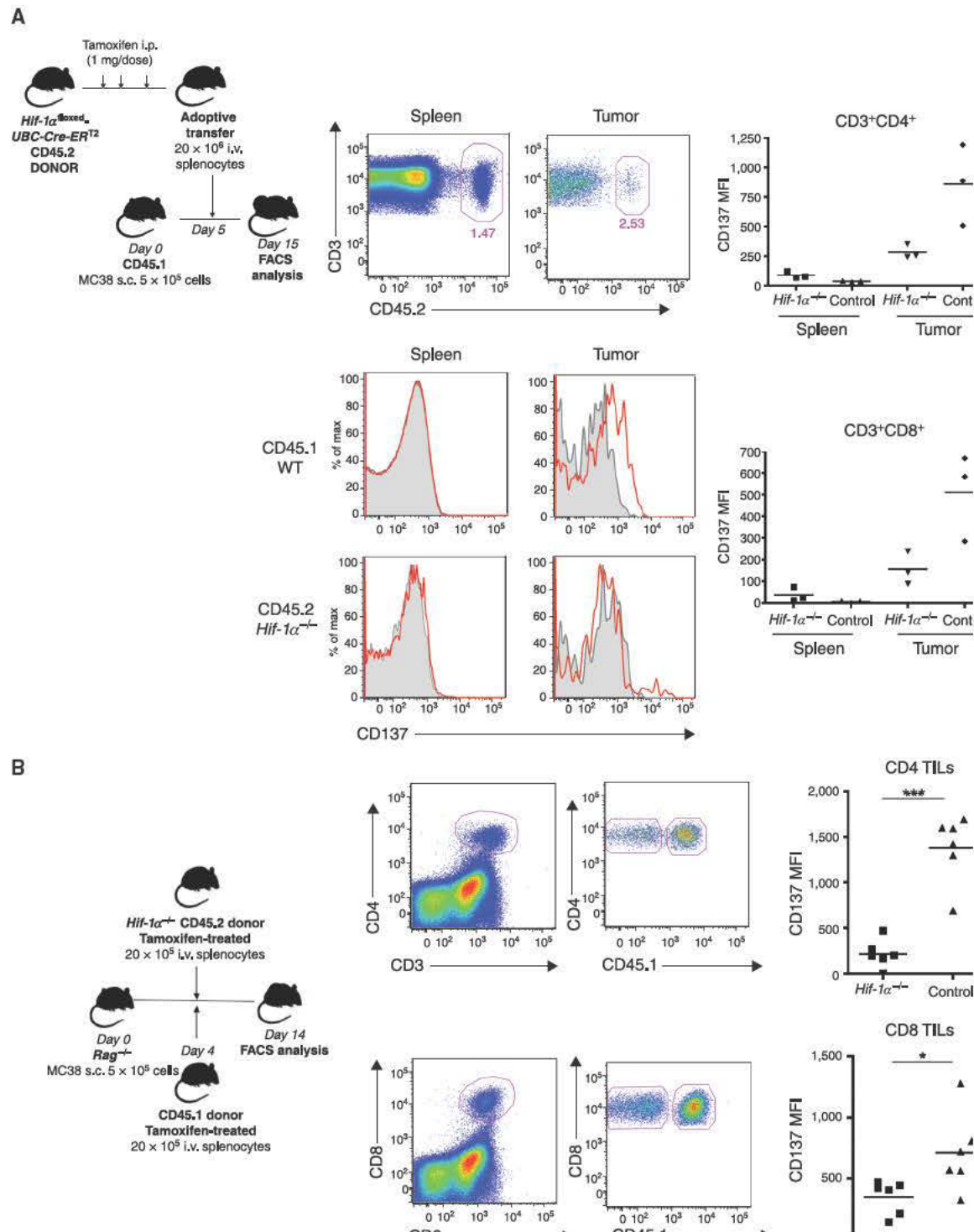


**Figure 5.** TILs upregulate CD137 in an *HIF-1 $\alpha$* -dependent fashion. **A**, *Hif-1 $\alpha$* <sup>flxed</sup>-*UBC-Cre-ERT2* mice homozygous for the CD45.2 allele were induced with tamoxifen for 5 days, checked for loss of HIF-1 $\alpha$ , and 1 week later, their splenocytes were adoptively transferred to congenic C57Bl/6 mice carrying the CD45.1 allele and bearing an established MC38-derived subcutaneous tumor. Ten days later, spleens and tumors were surgically excised and their CD45.1<sup>+</sup> and CD45.2<sup>+</sup> lymphocytes differentially analyzed by FACS. Dot plots show the gating strategy on CD3<sup>+</sup> T cells in the spleen and in the tumor as indicated. Representative histograms on CD45.1- and CD45.2-gated cells in the spleen and in CD3<sup>+</sup> TILs (tumor) are presented. Dot graphs show CD137-specific MFI in CD3<sup>+</sup>CD4<sup>+</sup> and CD3<sup>+</sup>CD8<sup>+</sup> T cells taken from the tumors or the spleens in 3 adoptively transferred mice. WT, wild-type. **B**, experiments as in **(A)** but in this case *Rag*<sup>-/-</sup> mice bearing MC38 tumors for 4 days were adoptively co-transferred with CD45.1 HIF-1 $\alpha$ -sufficient splenocytes from control mice pretreated with tamoxifen and with CD45.2 splenocytes from *Hif-1 $\alpha$* <sup>flxed</sup>-*UBC-Cre-ERT2* pre-induced with 4-hydroxytamoxifen (4-HT). Dot plots show the FACS gating strategy to distinguish CD45.1 positive and negative events between CD4 and CD8 TILs. Dot graphs represent the mean intensity of fluorescence specific for surface anti-CD137 immunostaining on CD4 and CD8 cells from gated CD45.1-positive and -negative TILs.

In conclusion, HIF-1 $\alpha$  in response to hypoxia plays a critical and necessary role in the induction of CD137 expression on TILs.

### Selective Expression of CD137 on TILs Can Be Exploited for Immunotherapy with Anti-CD137 Immunostimulatory mAb

The fact that CD137 expression is largely confined to the tumors could be exploited by intratumoral delivery of the agonist immunotherapeutic mAb. Intratumoral injections of as little as 5  $\mu$ g/dose of 1D8 mAb induced regressions in nearly half of CT26-bearing BALB/c mice treated when the tumors had already reached 5 mm in diameter (day 7).

Systemic treatment with anti-CD137 mAb and anti-B7-H1 (PD-L1) has been described to exert powerful synergistic effects (30). In this CT26 tumor model, repeated 100  $\mu$ g doses of anti-B7-H1 given intraperitoneally (i.p.) attained 5 of 12 complete regressions (Fig. 6A). Importantly, combined treatments of minute doses of anti-CD137 mAb given intratumorally and anti-B7-H1 mAb given systemically achieved complete regressions in 10 of 12 mice (Fig. 6A). These cured mice were immune to a rechallenge with CT26 cells 3 months later (Supplementary Fig. S7) as a result of systemic immune memory.

The effect of B7-H1 blockade is probably due to the fact that grafted CT26 cells forming the tumor mass express B7-H1 on the surface as described in other tumors (31). This is in contrast to the lack of expression on cultured CT26 cells, which can be induced to express B7-H1 by 48-hour culture in the presence of IFN- $\gamma$  (Fig. 6B). In conjunction with the expression of B7-H1 (PD-L1) on the tumor cells, CD4 and CD8 TILs express the checkpoint co-inhibitory molecule PD-1. Hence PD-1<sup>+</sup> TILs should be sensitive to depression by B7-H1 blockade (Fig. 6C). It was also found that PD-1<sup>bright</sup> TILs coincided with CD137<sup>+</sup> TILs. Taken together, these observations probably provide a reason for the synergistic effects of artificial costimulation via CD137 and simultaneous relief from PD-1 inhibition upon blockade of its ligand as previously described by Hirano and colleagues (30).

Importantly, low doses of anti-CD137 mAb achieved remarkable systemic therapeutic effects against concomitant established tumors. This was shown in a bilateral model of CT26-derived tumors transplanted on day 0 to one of the flanks and on day 4 to the opposite side to resemble metastatic disease. On days 7, 9, and 11, the primary lesion was intratumorally treated, whereas the smaller tumor was left untreated. As can be seen in Fig. 6D, 5 of these 7 distant tumor nodules underwent complete rejection, thus indicating the elicitation of concomitant antitumor immunity against tumor nodules that had not been directly treated with the 1D8 anti-CD137 mAb.

Absence of CD137 immunostaining on T cells in tumor-draining lymph nodes was confirmed (Supplementary Fig. S8), further suggesting that the therapeutic costimulatory events were taking place on the TILs. However, upon intratumoral treatment with low doses of 1D8 mAb, there was a clear hyperplasia of tumor-draining lymph nodes that became enlarged 3- to 4-fold over control IgG (Supplementary Fig. S9A).

In addition, the number of TILs increased upon intratumoral treatment with low-dose anti-CD137 mAb (Supplementary Fig. S9A). CD8<sup>+</sup> T cells increased both in terms of percentage and absolute numbers, whereas CD4<sup>+</sup> T cells decreased in absolute and relative numbers (Supplementary Fig. S9B and S9C). As a consequence of a decrease in CD4<sup>+</sup>FOXP3<sup>+</sup> T cells among TILs, a clear increase in the ratio of CD8 T cells/Treg was observed upon 1D8 mAb treatment (Supplementary Fig. S9D). It is of note that following intratumoral treatment, a tendency in the CD8<sup>+</sup> TILs to express higher levels of CD137, Granzyme B, and KLRG-1 was observed (Supplementary Fig. S9E). These results are in line with the observations reported by Curran and colleagues (32) upon systemic treatment with an anti-CD137 antibody. Also, consistent with a more active effector phenotype of such CD8 TILs, these T lymphocytes if restimulated *in vitro* with the AH1 tumor antigen peptide, expressed more IFN- $\gamma$  and TNF- $\alpha$  (Supplementary Fig. S10A–S10C).

### Safer Immunotherapy with Local Low Doses of Anti-CD137 mAb

Agonist anti-CD137 mAbs cause liver inflammation (25). One advantage of giving smaller and more localized doses of anti-CD137 mAb is that the side effects of CD137 known to be dose-dependent would be mitigated. In this regard, Fig. 7 shows that although three 100- $\mu$ g doses of anti-CD137 mAb given i.p. induced mild liver transaminase increases, 5  $\mu$ g given intratumorally 3 times did not cause this side effect (Fig. 7A). This is because CD8 T mononuclear cells do not accumulate forming inflammatory infiltrates in the liver of mice treated with the intratumoral 5- $\mu$ g doses (Fig. 7B–D). Importantly, combinatorial treatments with local anti-CD137 mAb and systemic anti-B7-H1 mAb do not cause liver inflammation (Fig. 7B–D). The idea of conducting intratumoral injections of lower doses of immunostimulatory mAbs had been previously applied successfully by Fransen and colleagues (33) with agonist anti-CD40 mAb. Their strategy also limits systemic toxicity while preserving antitumoral efficacy.

In our case with anti-CD137 mAb, we are exploiting the selective presence of the target for the immunostimulatory antibody at the hypoxic tumor microenvironment to spatially focus the immunotherapeutic effects while avoiding liver toxicity.

## DISCUSSION

Stromal components and malignant cells dialog and mutually change their functional responses. TILs are a prominent feature of malignant tissue whose presence has been correlated with a better survival outcome in various malignant diseases (34, 35). However, TILs are severely restrained in their ability to tackle tumor cells as a result of multifactorial immunosuppressive mechanisms, which are especially intense in the tumor microenvironment (36). Nonetheless, *ex vivo* cultures of TILs to expand and reinvigorate these cells have been used in adoptive cell therapy with reports of impressive objective responses in patients with melanoma (37).

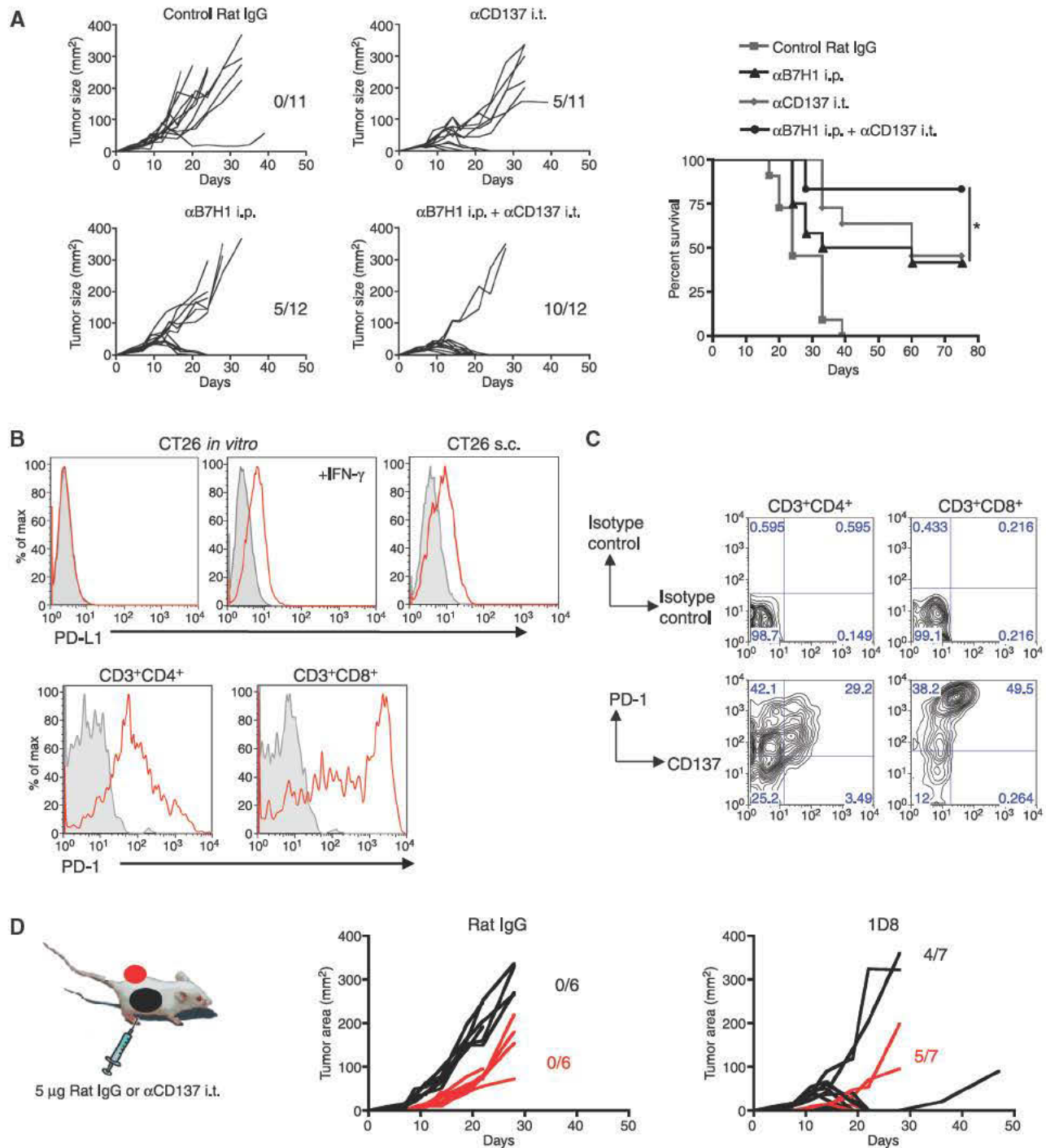


**Figure 6.** Intratumoral injections of small doses of agonist anti-CD137 mAb to directly act on CD137<sup>+</sup> TILs render systemic immunotherapeutic effects that are synergistic with PD-L1 (B7-H1) systemic blockade. **A**, mice bearing subcutaneous CT26 palpable tumors for 7 days were treated intratumorally with three 5- $\mu$ g doses of control rat IgG or anti-CD137 mAb on days 7, 9, and 11 or/and with 3 i.p. doses of 100  $\mu$ g anti-B7-H1 blocking mAb. Individual follow-up of tumor sizes is presented for each experimental group, the fraction of tumor-free mice at the end of the experiment is given in each graph, and the survival curves are presented. i.t., intratumorally. **B**, top, FACS histograms show that CT26 cells do not express B7-H1 in culture but are inducible by culture for 48 hours in the presence of IFN- $\gamma$  or when cells are freshly recovered from grafted tumors in syngeneic mice. Bottom FACS histograms show bright expression of PD-1 on CD3<sup>+</sup>CD4<sup>+</sup> and CD3<sup>+</sup>CD8<sup>+</sup> TILs harvested from CT26 tumors. **C**, dot plots showing CD137 and PD-1 double immunostainings on gated CD8<sup>+</sup> and CD4<sup>+</sup> T cells as indicated. Background immunostainings with isotype-matched control mAb tagged with the same fluorochromes are presented. **D**, BALB/c mice were subcutaneously inoculated with CT26 cells on days 0 and 4 in opposite flanks (black and red as indicated in schematic representation of the experiments). On days 7, 9, and 11, the primary tumor received intratumoral injections of 5  $\mu$ g of 1D8 mAb or control IgG. Graphs represent individual tumor sizes for the primary (black) and secondary (red) tumors. The fraction of mice completely rejecting tumors is provided with the corresponding black and red graphs.

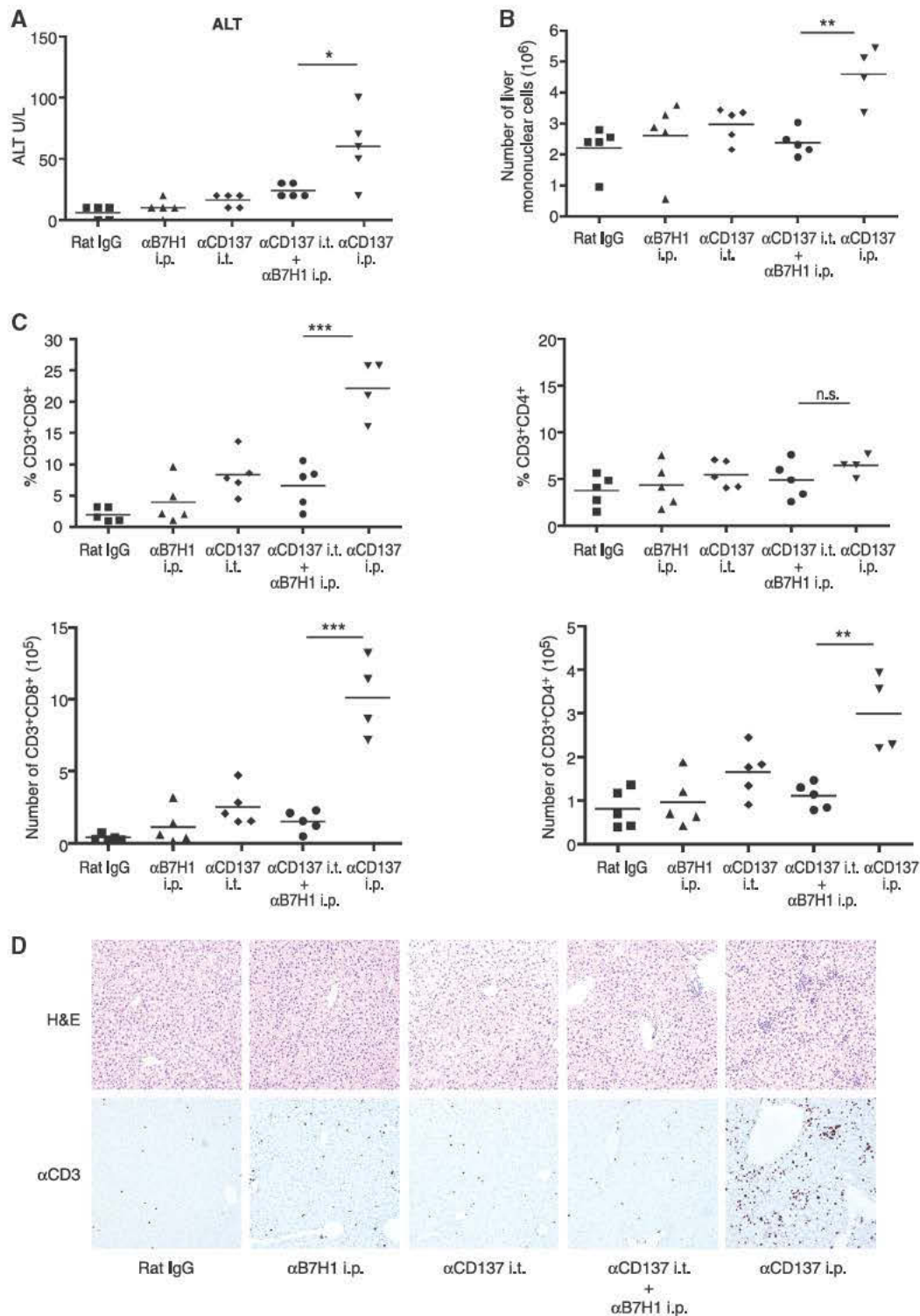


**Figure 7.** Low intratumoral doses of agonist anti-CD137 mAb do not cause liver inflammation. CT26 tumor-bearing mice (5 per group) were treated with the indicated mAbs either intratumorally or intraperitoneally. The i.p. injections consisted of 100  $\mu$ g per dose of mAb given on days 7, 9, 11; and intratumor (i.t.) injections in 5  $\mu$ g per dose given on days 7, 9, and 11. On day 18, mice were sacrificed, blood was drawn, livers were excised, and liver leukocytes were isolated in Percoll gradients. **A**, serum aminolevulinic transaminase serum concentration on day 18. ALT, alanine aminotransferase; \*,  $P < 0.05$ . **B**, the absolute number of mononuclear leukocytes recovered from the liver. \*\*,  $P < 0.01$ . **C**, the percentage (top graphs) and absolute numbers (bottom graphs) of CD4<sup>+</sup> and CD8<sup>+</sup> T cells in the liver as indicated for each group. n.s., not significant; \*\*\*,  $P < 0.001$ . **D**, representative microphotographs ( $\times 200$ ) of hematoxylin and eosin (H&E) stainings and CD3-specific immunohistochemistry of the indicated treatment groups.

Solid tumors are typically compromised in vascularization; as a result, they become hypoxic and respond by producing vascular growth factors to promote angiogenesis. Tumor hypoxia affects both malignant cells and stromal compartments presumably including infiltrating lymphocytes, although there is a conspicuous lack of information in this regard.

Hypoxia has been recently found to induce tumor cell production of a chemokine (CCL28) that attracts Tregs that would locally depress effector cellular immunity (38). However, very little is known about what tumor hypoxia does to tumor-infiltrating T cells directly. Experiments on T-cell cultures set up under hypoxia suggest a decrease in T-cell activation (39, 40), for instance, upon CD3/CD28 stimulation (39). The reasons could involve the HIF response to hypoxia and the effects of released adenosine that acts on inhibitory lymphocyte receptors for this moiety (1).

Moreover, a recent report involves HIF-1 transcription factors in the control of T-helper ( $T_H$ ) 17/Treg balance acting directly on T cells (41). Experiments on conditional HIF-1 $\alpha^{-/-}$  T cells indicate that the HIF-1 response downregulates acquisition of cytokine production and cytolytic activity in CD4 and CD8 T cells (42). Lack of detailed information about T-cell activation under low  $O_2$  tensions is worrying as immune responses in tissues occur at  $\geq 5\%$   $O_2$  (2) and tumors are even more hypoxic, at least in tissue regions located far from blood supply.

We had previously observed that the T-cell activation marker CD137 was upregulated on cultured endothelial cells as a result of hypoxia (8). Anti-CD137 mAb on these CD137 $^+$  endothelial cells elicited proinflammatory changes believed to be involved in the prominent immunotherapeutic effects of anti-CD137 agonist antibodies against tumors because of promoting homing of T lymphocytes to the tumor lesions.

In this study, we found that CD137 is upregulated on TILs but not in secondary lymphoid organs of tumor-bearing mice. Hypoxia was a candidate factor to explain CD137 expression on TILs. Indeed, grafted and spontaneous tumors are clearly hypoxic. However, hypoxia by itself does not induce CD137 on cultured T cells and TCR-CD3 stimulation is required. The striking finding is that CD137 is much more intensely upregulated on T cells undergoing activation when hypoxia is provided. Therefore, we can speculate that both antigen stimulation and hypoxia concurrently coexist in the tumor microenvironment to cooperatively give rise to CD137 expression on TILs. It is intriguing that NK lymphocytes in the tumor that ought to experience the same level of hypoxia do not upregulate CD137. Further studies will address the differential behavior of this lymphocyte subset which also expresses HIF-1 $\alpha$  mRNA.

Hypoxia causes various cellular changes such as induction of functionality of HIF-1 $\alpha$  and HIF-2 transcription factors, generation of free radicals, and adenosine release to the surrounding milieu (1). To ascertain which hypoxia response was involved in CD137 upregulation, we carried out compelling experiments using T cells from HIF-1 $\alpha$ -inducible knockout mice. Such T cells upregulate CD137 much less efficiently when undergoing activation

under hypoxia. Accordingly, experiments in which HIF-1 $\alpha$ -deficient and -sufficient T cells co-infiltrate tumors show that CD137 is selectively expressed on the hypoxia-responsive lymphocytes.

We considered the possibility that CD137 was a direct transcriptional target of HIF-1 $\alpha$ /1 $\beta$ , but detailed bioinformatic analyses of the *cd137* locus did not reveal any interspecies-conserved hypoxia response elements in the noncoding regions 10 kb upstream and downstream of the *cd137* locus including introns (43). Hence, the alternative hypothesis of indirect CD137 enhancing effects mediated by genes upregulated by the transcriptional activity of HIF-1 $\alpha$  is under investigation. In fact, previous reports have revealed a functional interplay of HIF-1 $\alpha$  and NF- $\kappa$ B members (44), whereas canonical NF- $\kappa$ B sites are leading inducers of the CD137 promoter (10). In fact, CD137 upregulation in our experiments seems to take place mainly at the transcriptional level. An antecedent for indirect effects exerted by HIF-1 $\alpha$  in T cells has been recently published by Dang and colleagues (41), who unraveled unexpected functions of HIF-1 $\alpha$  that are critical for the immune system such as protein-to-protein regulation of FOXP3 degradation in CD4 T cells and the control of the expression of secondary transcription factors.

We cannot be sure that cognate antigen and HIF-1 $\alpha$  response are the only factors behind CD137 expression on TILs, but our adoptive transfer experiments with HIF-1 $\alpha$ -deficient T cells clearly indicate that HIF-1 $\alpha$  is a critical factor for CD137 upregulation on TILs. The contribution of hypoxia to CD137 expression on T lymphocytes *in vivo* might extend to other hypoxia situations such as tissues destroyed by infection or atherosclerotic lesions.

The fact that CD137 is a target for a powerful strategy of immunostimulation against cancer makes the observation that TILs are selectively expressing CD137 very appealing. However, the tumor microenvironment is a difficult place for T-cell stimulation because of the abundance of immunoinhibitory factors. Among these suppressive factors, the PD-1/B7-H1 (PD-L1) pathway stands out as hierarchically very important (45, 46). The importance is highlighted by the fact that its blockade is immunotherapeutic in mice and humans (47).

Tregs are perceived also as an important repressor of therapeutic immunity against tumors. We found that CD4 $^+$ FOXP3 $^+$  lymphocytes among TILs express CD137 and would be able to interact with injected anti-CD137 mAb. The effect of CD137 stimulation on Tregs has been reported as dual because despite promoting Treg proliferation, Treg exposure to agonist anti-CD137 mAb weakens the suppressor activities and also desensitizes effector T lymphocytes to the suppressor effects (48). In our study, we confirm bright expression on these suppressive lymphocytes; but in our hands, sensing hypoxia via HIF-1 $\alpha$  is not a prominent driving factor for their expression of CD137.

Agonist anti-CD137 mAbs as monotherapy attain impressive responses against many transplanted tumors, although some of these are resistant including spontaneous breast carcinomas in MMTV-*Neu* mice (20, 49). Although treated mice survive curative anti-CD137 mAb treatments without signs of distress, transient liver inflammation and

myelosuppression have been reported in repeatedly treated animals (26). Fransen and colleagues (33) showed that anti-CD40 mAb at low doses inside tumors can be efficacious without systemic toxicity. We have found that because of the selective presence of CD137 on TILs, the effect of the antibody can be delivered locally without liver inflammation. Importantly, CD137 delivered intratumorally is synergistic with B7-H1 blockade; this synergy had been previously described by Hirano and colleagues (30). Studies in mice chronically infected with LCMV also show synergistic therapeutic effects of anti-CD137 and anti-B7-H1 mAb that correlate with an enhancement of CD8-mediated antiviral immunity (50). Combinatorial treatments with systemic B7-H1 blockade and local agonist anti-CD137 mAbs are highly efficacious. This probably reflects that the very same TILs released from PD-1 inhibition are being provided costimulation via CD137. Importantly, local injection of anti-CD137 mAb attained systemic therapeutic effects against concomitant tumors that are postulated to be mediated by recirculation of the properly stimulated TILs.

Recently, an elegant report from Alizadeh and colleagues (51) has shown that TILs in human lymphomas express surface CD137 and that the amount of CD137 on human pathology specimens of this malignancy correlated favorably with prognosis. Further research should extend these observations to TILs in other human tumors and study a potential correlation with hypoxia.

In summary, CD137 is expressed on TILs because of a response to hypoxia mediated by HIF-1 $\alpha$ . The physiologic reason behind these facts is unknown, but it can be exploited to target CD137 stimulation to where it is most needed, thus limiting systemic side effects. Combinatorial PD-L/B7-H1 (PD-1) pathway blockade and anti-CD137 local stimulation offer many potential clinical advantages, and human immunostimulatory mAbs to all these targets are being tested (24).

## METHODS

### Mice and Cell Lines

BALB/c and C57/BL6 wild-type mice (5 to 6 weeks old) were purchased from Harlan Laboratories. OT-1, OT-2, CD45.1, *Rag*<sup>-/-</sup>, and MMTV-*NeuT* mice (52) were purchased from the Jackson Laboratory and bred in our animal facility under specific pathogen-free conditions. CD137<sup>-/-</sup> mice in pure BALB/c background have been previously described (8).

*Hif-1 $\alpha$* <sup>flxed</sup>-*UBC-Cre-ER*<sup>T2</sup> mice were generated from B6.129-*Hif-1 $\alpha$* <sup>tm3Rsj/J</sup> mice (Jackson Laboratories, stock no. 007561), which harbor 2 *loxP* sites flanking exon 2 of the murine *Hif-1 $\alpha$*  locus. These mice were crossed with *Tg(UBC-Cre/ER*<sup>T2</sup>*)IEjbj* mice (Jackson Laboratories, stock no. 008085) as described above to generate *Hif-1 $\alpha$* <sup>flxed</sup>-*UBC-Cre-ER*<sup>T2</sup> mice and their corresponding controls, *Hif-1 $\alpha$* <sup>wt</sup>-*UBC-Cre-ER*<sup>T2</sup> and *Hif-1 $\alpha$* <sup>flxed</sup> mice. For *Hif-1 $\alpha$*  gene inactivation, *Hif-1 $\alpha$* <sup>flxed</sup>-*UBC-Cre-ER*<sup>T2</sup> and the corresponding control mice (10 to 15 weeks old) were treated with 3 every other day i.p. doses (total of 3 doses) of 1 mg of 4-hydroxytamoxifen (Merck); 7 days after the last dose, the animals were used for experiments. All animal procedures were conducted under Institutional Guidelines that comply with National Laws and Policies (study approval 070-10).

CT26, B16-OVA, and MC38 tumor cell lines were from American Type Culture Collection and the master cell banks authenticated in 2011 by RADIL (Case Number: 6592-2012). Cells were cultured in complete RPMI medium [RPMI-1640 with GlutaMAX (Gibco)

containing 10% heat-inactivated FBS (Sigma-Aldrich), 100 IU/mL penicillin, and 100  $\mu$ g/mL streptomycin (BioWhittaker) and 5  $\times$  10<sup>-5</sup> mol/L 2-mercaptoethanol (Gibco)]. For hypoxic culture conditions, splenocytes were incubated for the indicated times under 1% O<sub>2</sub> atmosphere in a modular incubator chamber (Billups-Rothenberg Inc.) or the H35 Hypoxystation (Don Whitley) for those experiments in which retrieval of part of the cultures from hypoxia was required.

### Human T-cell Experiments

Anonymous buffy coat by-products of blood donations were procured under informed consent of the donors and under approval of the regional committee of ethics of the local government of Navarra. PBMCs were prepared by Ficoll gradients and T cells were stimulated in 6-well plates precoated with 1  $\mu$ g/mL of OKT3 mAb in the same culture medium as in the mouse experiments but without 2-mercaptoethanol. Forty-eight cultures were placed under hypoxia (1% O<sub>2</sub>) or in the presence of 0.2 mmol/L of DMOG when indicated. Retrieved cells were analyzed by flow cytometry upon multicolor immunostaining with fluorochrome anti-CD3, CD4, CD8 (Becton Dickinson) and CD137 (e-bioscience)-specific mAb.

### In Vivo Tumor Growth

A total of 0.5  $\times$  10<sup>6</sup> CT26, MC38, or B16-OVA cells were injected subcutaneously into the flank in 100  $\mu$ L PBS. Mice and tumor size were monitored and mice were sacrificed when tumor size reached 300 mm<sup>2</sup> (53). For some experiments, mice were injected bilaterally in opposite flanks with 0.5  $\times$  10<sup>6</sup> CT26 tumor cells with a delay of 4 days between sites. In those experiments, only the larger primary tumor was injected with the antibody.

### Flow Cytometry, Antibodies, and Tissue Immunofluorescence

For immunofluorescence and flow cytometric analyses of TILs, cleanly excised tumor nodules were placed in Petri dishes, minced finely with a scalpel blade, and incubated for 25 minutes at 37°C in a solution containing Collagenase-D and DNase-I (Roche) in RPMI. The entire material was passed through a 70- $\mu$ m cell strainer (BD Falcon, BD Bioscience) and pressed with a plunger to obtain unicellular cell suspensions. Single-cell suspensions were pretreated with FcR-Block (anti-CD16/32 clone 2.4G2; BD Biosciences-Pharmingen). Afterward, cells were stained with the following antibodies or reagents obtained from BD Pharmingen: CD3, CD4, CD8, CD137, CD49b, CD45.1, PD-1, PD-L1, KLRG-1, F4/80, Gr-1, CD11b, CD11c, Granzyme B, FOXP3, TNF- $\alpha$ , IFN- $\gamma$ , and/or the respective conjugated isotype controls. For TNF- $\alpha$  and IFN- $\gamma$  intracellular staining, tumor mononuclear cells were restimulated with AH1 peptide (SPSYVYHQF 10  $\mu$ g/mL, NeoMPS) for 1 hour and incubated overnight in the presence of brefeldin-A (10  $\mu$ g/mL; Sigma) and then fixed and permeabilized with Fix/perm buffer (eBiosciences) before FACS staining. OT-1 and OT-2 peptides were also from NeoMPS.

FACSCanto II and FACSCalibur (BD Pharmingen) as indicated were used for cell acquisition and data analysis was carried out using FlowJo (TreeStar software).

The hybridomas producing agonistic mouse anti-CD137 (clone 2A) and anti-B7-H1 (PD-L1; clone 10B5) were kindly provided by Dr. Lieping Chen (Yale University, New Haven, CT). Mean fluorescence intensity (MFI) values represent the subtraction of specific versus control MFI. Polyclonal rat IgG with undetectable lipopolysaccharide (LPS; Sigma) was used as control. Mouse anti-CD3/CD28 microbeads were from Dynabeads (Invitrogen). DMOG was purchased from Enzo Life Sciences.

Tissue immunofluorescence staining was conducted on 10- $\mu$ m thick cryosections with the following antibodies: CD4, CD8

(eBiosciences) and goat anti-CD137 (R&D Systems) followed by anti-goat AF488 (Invitrogen) as a secondary antibody. For confocal microscopy, LSM 510 META (Carl Zeiss) equipment was used. The images were analyzed using Zeiss LSM Image Browser software.

### Small-Animal PET Analyses

Tumor hypoxia was measured by PET with the radiotracer fluorine-18-fluoromisonidazole (<sup>18</sup>F-FMISO). On the day of the study, mice were anesthetized with 2% isoflurane in 100% O<sub>2</sub> gas for <sup>18</sup>F-FMISO injection (14.9 ± 4.9 MBq in 100 μL) in the tail vein. Four hours after the tracer injection, mice were placed prone on the PET scanner. A static 30-minute study (sinogram) was acquired using a Mosaic (Philips) small-animal dedicated imaging tomography with 11.9 cm axial field of view (FOV) and 12.8 cm transaxial FOV and a 2-mm resolution. Images were reconstructed using the 3-dimensional (3D) Ramla algorithm (a true 3D reconstruction) with 2 iterations and a relaxation parameter of 0.024 into a 128 × 128 matrix with a 1-mm voxel size applying dead time, decay, random, and scattering corrections.

For the assessment of tumor <sup>18</sup>F-FMISO uptake, all studies were exported and analyzed using the PMOD software (PMOD Technologies Ltd.). Regions of interest were drawn on coronal 1-mm thick small-animal PET images on consecutive slices including the entire tumor. Finally, maximum standardized uptake value (SUV) was calculated for each tumor using the formula  $SUV = [\text{tissue activity concentration (Bq/cm}^3\text{)}/\text{injected dose (Bq)}] \times \text{body weight (g)}$ .

### Molecular Analyses

Total RNA was extracted from lymphocytes using the RNeasy Mini Kit (Qiagen). We treated RNA with DNaseI (Gibco-BRL) before reverse transcription with M-MLV reverse transcriptase (Gibco-BRL) in the presence of RNaseOUT (Gibco-BRL). Real-time PCR was carried out with iQ SYBR green supermix in an iQ5 real-time PCR detection system (Bio-Rad). Copy numbers of CD137 cDNA were quantified by quantitative PCR with primers annealing the mouse CD137 cDNA (forward primer, 5'-AACATCTGCAGAGTGTGTGC-3'; reverse primer, 5'-AGACCTCCGTCTAGAGAGC-3'; product length, 252 bp). Samples were analyzed in triplicate, and data were normalized by comparison with β-actin as an internal control (forward primer, 5'-CGCGTCCACCCGCGAG-3'; reverse primer, 5'-CCTGGTGCCTAGGGCG-3'; product length, 194 bp). The amount of each transcript was expressed according to the formula  $2^{-C_t(\beta\text{-actin}) - \Delta C_t(\text{CD137})}$ , where  $C_t$  is the cycle at which the fluorescence increases appreciably above background fluorescence.

### Adoptive T-cell Transfers

*Hif-1α*<sup>flloxed</sup>.*UBC-Cre-ER*<sup>T2</sup> or CD45.1 donor mice were treated with tamoxifen. One week later, total splenocytes were inoculated intravenously (10<sup>7</sup> spleen cells per mouse) into CD45.1 or *Rag*<sup>-/-</sup> recipient mice carrying subcutaneous MC38 tumors. Ten days following T-cell transfer, tumors were harvested and analyzed for CD137 expression on CD45.1 versus CD45.2 T cells in a FACSCanto II flow cytometer.

### Statistical Analysis

Prism software (GraphPad Software) was used to determine statistical significance of the differences between groups by applying the unpaired Student *t* tests or 2-way ANOVA tests. *P* values of <0.05 were considered significant.

### Disclosure of Potential Conflicts of Interest

M. Jure-Kunkel is a full-time employee of Bristol-Myers Squibb, I. Melero is a consultant for Bristol-Myers Squibb, Merck-Serono, Pfizer Inc., Miltenyi Biotec, and DIGNA-Biotech and has Ownership

Interest (including patents) in Bristol-Myers Squibb. No potential conflicts of interests were disclosed by the other authors.

### Authors' Contributions

**Conception and design:** A. Palazón, I. Martínez-Forero, J.L. Perez-Gracia, S. Hervás-Stubbs, I. Melero

**Development of methodology:** A. Palazon, A. Morales-Kastresana, C. Alfaro, J.L. Perez-Gracia, S. Hervás-Stubbs, A. Rouzaut, J. Aragonés

**Acquisition of data (provided animals, acquired and managed patients, provided facilities, etc.):** A. Palazón, I. Martínez-Forero, A. Teijeira, I. Peñuelas, A. Rouzaut, M.O. de Landázuri, M. Jure-Kunkel, J. Aragonés

**Analysis and interpretation of data (e.g., statistical analysis, biostatistics, computational analysis):** A. Palazón, I. Martínez-Forero, C. Alfaro, J.L. Perez-Gracia, I. Melero

**Writing, review, and/or revision of the manuscript:** A. Palazon, M.F. de Sanmamed, J.L. Perez-Gracia, M. Jure-Kunkel, I. Melero

**Administrative, technical, or material support (i.e., reporting or organizing data, constructing databases):** A. Palazón, C. Alfaro

**Study supervision:** S. Hervás-Stubbs, I. Melero

**Carried out all experiments:** A. Palazón

### Acknowledgments

The authors acknowledge long-term collaborations on CD137 with Dr. Lieping Chen (Johns Hopkins, Baltimore, MD) and scientific discussion with Dr. Luis del Peso (Universidad Autónoma de Madrid, Madrid, Spain) and Dr. Jesus Prieto (Universidad de Navarra, Navarra, Spain); excellent animal care by Eneko Elizalde and Elena Ciordea; flow cytometric assistance by Dr. Diego Alignani; and English editing by Dr. Paul Miller.

### Grant Support

The financial support was obtained from MEC/MICINN (SAF2005-03131 and SAF2008-03294), Departamento de Educación del Gobierno de Navarra, Departamento de Salud del Gobierno de Navarra; Redes temáticas de investigación cooperativa RETIC (RD06/0020/0065), European commission VII framework program (ENCITE), SUDOE-IMMUNONET, and "UTE for project FIMA". S. Hervás-Stubbs has a Ramon y Cajal contract from MICINN and A. Palazón a scholarship from FIS. A. Morales-Kastresana receives an FPI scholarship from MICINN.

Received November 28, 2011; revised April 23, 2012; accepted April 25, 2012; published OnlineFirst June 19, 2012.

### REFERENCES

1. Sitkovsky MV, Lukashev D, Apasov S, Kojima H, Koshiba M, Caldwell C, et al. Physiological control of immune response and inflammatory tissue damage by hypoxia-inducible factors and adenosine A2A receptors. *Annu Rev Immunol* 2004;22:657-82.
2. Caldwell CC, Kojima H, Lukashev D, Armstrong J, Farber M, Apasov SG, et al. Differential effects of physiologically relevant hypoxic conditions on T lymphocyte development and effector functions. *J Immunol* 2001;167:6140-9.
3. Palazon A, Aragonés J, Morales-Kastresana A, de Landázuri MO, Melero I. Molecular pathways: hypoxia response in immune cells fighting or promoting cancer. *Clin Cancer Res* 2012;18: 1207-13.
4. Semenza GL. Life with oxygen. *Science* 2007;318:62-4.
5. Aragonés J, Fraisl P, Baes M, Carmeliet P. Oxygen sensors at the crossroad of metabolism. *Cell Metab* 2009;9:11-22.

6. Jaakkola P, Mole DR, Tian YM, Wilson MI, Gielbert J, Gaskell SJ, et al. Targeting of HIF- $\alpha$  to the von Hippel-Lindau ubiquitylation complex by O<sub>2</sub>-regulated prolyl hydroxylation. *Science* 2001; 292:468–72.
7. Ivan M, Kondo K, Yang H, Kim W, Valiano J, Ohh M, et al. HIF $\alpha$  targeted for VHL-mediated destruction by proline hydroxylation: implications for O<sub>2</sub> sensing. *Science* 2001;292:464–8.
8. Palazon A, Teixeira A, Martinez-Forero I, Hervas-Stubbs S, Roncal C, Penuelas I, et al. Agonist anti-CD137 mAb act on tumor endothelial cells to enhance recruitment of activated T lymphocytes. *Cancer Res* 2011;71:801–11.
9. Pollok KE, Kim YJ, Zhou Z, Hurtado J, Kim KK, Pickard RT, et al. Inducible T cell antigen 4-1BB. Analysis of expression and function. *J Immunol* 1993;150:771–81.
10. Imam SK. Review of positron emission tomography tracers for imaging of tumor hypoxia. *Cancer Biother Radiopharm* 2010; 25:365–74.
11. Watts TH. TNF/TNFR family members in costimulation of T cell responses. *Annu Rev Immunol* 2005;23:23–68.
12. Melero I, Johnston JV, Shufford WW, Mittler RS, Chen L. NK1.1 cells express 4-1BB (CDw137) costimulatory molecule and are required for tumor immunity elicited by anti-4-1BB monoclonal antibodies. *Cell Immunol* 1998;190:167–72.
13. Choi BK, Kim YH, Kwon PM, Lee SC, Kang SW, Kim MS, et al. 4-1BB functions as a survival factor in dendritic cells. *J Immunol* 2009;182:4107–15.
14. Drenkard D, Becke FM, Langstein J, Spruss T, Kunz-Schughart LA, Tan TE, et al. CD137 is expressed on blood vessel walls at sites of inflammation and enhances monocyte migratory activity. *FASEB J* 2007;21:456–63.
15. Tan JT, Whitmire JK, Ahmed R, Pearson TC, Larsen CP. 4-1BB ligand, a member of the TNF family, is important for the generation of antiviral CD8 T cell responses. *J Immunol* 1999;163:4859–68.
16. Kwon BS, Hurtado JC, Lee ZH, Kwack KB, Seo SK, Choi BK, et al. Immune responses in 4-1BB (CD137)-deficient mice. *J Immunol* 2002;168:5483–90.
17. Melero I, Shufford WW, Newby SA, Aruffo A, Ledbetter JA, Hellstrom KE, et al. Monoclonal antibodies against the 4-1BB T-cell activation molecule eradicate established tumors. *Nat Med* 1997;3:682–5.
18. Wilcox RA, Chapoval AI, Gorski KS, Otsuji M, Shin T, Flies DB, et al. Cutting edge: expression of functional CD137 receptor by dendritic cells. *J Immunol* 2002;168:4262–7.
19. Mittler RS, Foell J, McCausland M, Strahotin S, Niu L, Bapat A, et al. Anti-CD137 antibodies in the treatment of autoimmune disease and cancer. *Immunol Res* 2004;29:197–208.
20. Melero I, Murillo O, Dubrot J, Hervas-Stubbs S, Perez-Gracia JL. Multi-layered action mechanisms of CD137 (4-1BB)-targeted immunotherapies. *Trends Pharmacol Sci* 2008;29:383–90.
21. McNamara JO, Kolonias D, Pastor F, Mittler RS, Chen L, Giangrande PH, et al. Multivalent 4-1BB binding aptamers costimulate CD8<sup>+</sup> T cells and inhibit tumor growth in mice. *J Clin Invest* 2008;118:376–86.
22. Yang Y, Yang S, Ye Z, Jaffar J, Zhou Y, Cutter E, et al. Tumor cells expressing anti-CD137 scFv induce a tumor-destructive environment. *Cancer Res* 2007;67:2339–44.
23. Murillo O, Dubrot J, Palazon A, Arina A, Azpilikueta A, Alfaro C, et al. *In vivo* depletion of DC impairs the anti-tumor effect of agonistic anti-CD137 mAb. *Eur J Immunol* 2009;39:2424–36.
24. Ascierto PA, Simeone E, Sznol M, Fu YX, Melero I. Clinical experiences with anti-CD137 and anti-PD1 therapeutic antibodies. *Semin Oncol* 2010;37:508–16.
25. Dubrot J, Milheiro F, Alfaro C, Palazon A, Martinez-Forero I, Perez-Gracia JL, et al. Treatment with anti-CD137 mAbs causes intense accumulations of liver T cells without selective antitumor immunotherapeutic effects in this organ. *Cancer Immunol Immunother* 2010;59:1223–33.
26. Niu L, Strahotin S, Hewes B, Zhang B, Zhang Y, Archer D, et al. Cytokine-mediated disruption of lymphocyte trafficking, hemopoiesis, and induction of lymphopenia, anemia, and thrombocytopenia in anti-CD137-treated mice. *J Immunol* 2007;178:4194–213.
27. Ryan HE, Lo J, Johnson RS. HIF-1  $\alpha$  is required for solid tumor formation and embryonic vascularization. *EMBO J* 1998; 17:3005–15.
28. Feil R, Wagner J, Metzger D, Chambon P. Regulation of Cre recombinase activity by mutated estrogen receptor ligand-binding domains. *Biochem Biophys Res Commun* 1997;237:752–7.
29. Miro-Murillo M, Elorza A, Soro-Araiz I, Albacete-Albacete L, Ordóñez A, Balsa E, et al. Acute Vhl gene inactivation induces cardiac HIF-dependent erythropoietin gene expression. *PLoS One* 2011;6:e22589.
30. Hirano F, Kaneko K, Tamura H, Dong H, Wang S, Ichikawa M, et al. Blockade of B7-H1 and PD-1 by monoclonal antibodies potentiates cancer therapeutic immunity. *Cancer Res* 2005;65:1089–96.
31. Dong H, Strome SE, Salomao DR, Tamura H, Hirano F, Flies DB, et al. Tumor-associated B7-H1 promotes T-cell apoptosis: a potential mechanism of immune evasion. *Nat Med* 2002;8:793–800.
32. Curran MA, Kim M, Montalvo W, Al-Shamkhani A, Allison JP. Combination CTLA-4 blockade and 4-1BB activation enhances tumor rejection by increasing T-cell infiltration, proliferation, and cytokine production. *PLoS One* 2011;6:e19499.
33. Fransen MF, Sluijter M, Morreau H, Arens R, Melief CJ. Local activation of CD8 T cells and systemic tumor eradication without toxicity via slow release and local delivery of agonistic CD40 antibody. *Clin Cancer Res* 2011;17:2270–80.
34. Zhang L, Conejo-Garcia JR, Katsaros D, Gimotty PA, Massobrio M, Regnani G, et al. Intratumoral T cells, recurrence, and survival in epithelial ovarian cancer. *N Engl J Med* 2003;348:203–13.
35. Galon J, Fridman WH, Pages F. The adaptive immunologic microenvironment in colorectal cancer: a novel perspective. *Cancer Res* 2007;67:1883–6.
36. Drake CG, Jaffee E, Pardoll DM. Mechanisms of immune evasion by tumors. *Adv Immunol* 2006;90:51–81.
37. Rosenberg SA. Cell transfer immunotherapy for metastatic solid cancer—what clinicians need to know. *Nat Rev Clin Oncol* 2011;8: 577–85.
38. Facciabene A, Peng X, Hagemann IS, Balint K, Barchetti A, Wang LP, et al. Tumour hypoxia promotes tolerance and angiogenesis via CCL28 and T(reg) cells. *Nature* 2011;475:226–30.
39. Atkuri KR, Herzenberg LA, Niemi AK, Cowan T. Importance of culturing primary lymphocytes at physiological oxygen levels. *Proc Natl Acad Sci U S A* 2007;104:4547–52.
40. Atkuri KR, Herzenberg LA. Culturing at atmospheric oxygen levels impacts lymphocyte function. *Proc Natl Acad Sci U S A* 2005;102: 3756–9.
41. Dang EV, Barbi J, Yang HY, Jinasena D, Yu H, Zheng Y, et al. Control of T(H)17/T(reg) balance by hypoxia-inducible factor 1. *Cell* 2011;146:772–84.
42. Lukashev D, Klebanov B, Kojima H, Grinberg A, Ohta A, Berenfeld L, et al. Cutting edge: hypoxia-inducible factor 1 $\alpha$  and its activation-inducible short isoform I.1 negatively regulate functions of CD4<sup>+</sup> and CD8<sup>+</sup> T lymphocytes. *J Immunol* 2006;177: 4962–5.
43. Ortiz-Barahona A, Villar D, Pescador N, Amigo J, del Peso L. Genome-wide identification of hypoxia-inducible factor binding sites and target genes by a probabilistic model integrating transcription-profiling data and *in silico* binding site prediction. *Nucleic Acids Res* 2010; 38:2332–45.
44. Taylor CT. Interdependent roles for hypoxia inducible factor and nuclear factor-kappaB in hypoxic inflammation. *J Physiol* 2008; 586:4055–9.
45. Sakuishi K, Apetoh L, Sullivan JM, Blazar BR, Kuchroo VK, Anderson AC. Targeting Tim-3 and PD-1 pathways to reverse T cell exhaustion and restore anti-tumor immunity. *J Exp Med* 2011;207: 2187–94.
46. Wang S, Chen L. Immunobiology of cancer therapies targeting CD137 and B7-H1/PD-1 cosignal pathways. *Curr Top Microbiol Immunol* 2011;344:245–67.

47. Brahmer JR, Drake CG, Wollner I, Powderly JD, Picus J, Sharfman WH, et al. Phase I study of single-agent anti-programmed death-1 (MDX-1106) in refractory solid tumors: safety, clinical activity, pharmacodynamics, and immunologic correlates. *J Clin Oncol* 2010; 28:3167-75.
48. So T, Lee SW, Croft M. Immune regulation and control of regulatory T cells by OX40 and 4-1BB. *Cytokine Growth Factor Rev* 2008; 19:253-62.
49. Dubrot J, Palazon A, Alfaro C, Azpilikueta A, Ochoa MC, Rouzaut A, et al. Intratumoral injection of interferon-alpha and systemic delivery of agonist anti-CD137 monoclonal antibodies synergize for immunotherapy. *Int J Cancer* 2011;128:105-18.
50. Vezyz V, Penaloza-Macmaster P, Barber DL, Ha SJ, Konieczny B, Freeman GJ, et al. 4-1BB signaling synergizes with programmed death ligand 1 blockade to augment CD8 T cell responses during chronic viral infection. *J Immunol* 2011;187:1634-42.
51. Alizadeh AA, Gentles AJ, Alencar AJ, Liu CL, Kohrt HE, Houot R, et al. Prediction of survival in diffuse large B-cell lymphoma based on the expression of 2 genes reflecting tumor and microenvironment. *Blood* 2011;118:1350-8.
52. Boggio K, Nicoletti G, Di Carlo E, Cavallo F, Landuzzi L, Melani C, et al. Interleukin 12-mediated prevention of spontaneous mammary adenocarcinomas in two lines of Her-2/neu transgenic mice. *J Exp Med* 1998;188:589-96.
53. Tirapu I, Arina A, Mazzolini G, Duarte M, Alfaro C, Feijoo E, et al. Improving efficacy of interleukin-12-transfected dendritic cells injected into murine colon cancer with anti-CD137 monoclonal antibodies and alloantigens. *Int J Cancer* 2004;110:51-60.